Title: ABA-induced MYB transcriptional module regulates the differentiation trajectory of chickpea exodermis

Authors: Leonardo Jo[1,2], Rianne Kluck[1], Sara Buti[1], Julia Holbein[2], Himanshu Chhillar[3], Pingtao Ding[3], Rochus Benni Franke[2], Kaisa Kajala[1]*

[1] Experimental & Computational Plant Development, Institute of Environmental Biology, Utrecht University, Utrecht, the Netherlands

[2] Current Affiliation: Laboratory of Molecular Biology, Wageningen University & Research, Droevendaalsesteeg 1, 6708PB, Wageningen, The Netherlands.

[3] Institute of Cellular and Molecular Botany, Rheinische Friedrich-Wilhelms-University of Bonn, Bonn, Germany.

[4] Institute of Biology Leiden, Leiden University, Leiden, the Netherlands.

* Corresponding author, k.kajala@uu.nl

Abstract

Abscisic acid (ABA) regulates plant responses to stress and influences the differentiation of root barrier cell types, such as the endodermis and exodermis. Despite the importance of the exodermis in limiting water and solute fluxes, its regulation remains poorly understood in legumes. Here, we characterize the ABA-induced suberization and lignification of root tissues across eight galegoid legumes. Chickpea exhibited suberin deposition specifically in the outermost cortex, forming a functional apoplastic barrier. Transcriptomics of chickpea roots revealed ABA-induced programs that were temporally separated, specifically, a rapid program with the general ABA response, and a delayed program of suberin biosynthesis. We identified putative MYB transcription factors that link the ABA response to the suberin biosynthesis in chickpea. Single-cell RNA-seq of chickpea roots uncovered putative cell-type-specific regulatory networks, suggesting that ABA-induced suberization in the exodermis is mediated by the canonical ABA signaling inducing the expression of suberin-regulating MYBs.

Introduction

Plants exhibit indeterminate and highly plastic growth, allowing them to adjust their development in response to fluctuating environmental conditions. This plasticity extends to the differentiation trajectories of individual plant cells, which are not solely determined by developmental programs but also integrate environmental signals to modify their structure and function. One of the key stress cues in plants is abscisic acid (ABA), a plant hormone that regulates many responses to drought, salinity, and other abiotic stressors. ABA has been shown to influence the differentiation of various root cell types, including the endodermis and the exodermis, whose differentiation program that deposits suberin lamella (SL) into the cell walls is induced by ABA[1–5]. SL add to the diffusion barrier properties of these cell types and help with retention of water and likely oxygen[3,5,6]. Notably, endodermis and exodermis also have a second differentiation program that deposits localized lignin into their cell walls, and this program is in many species under developmental control[7–14]. The endodermal lignin is precisely positioned and forms the Casparian strip that divides the endodermal cells to soil-facing and vasculature-facing sides and functions as an apoplastic diffusion barrier between the two. This provides the endodermis the ability to be a selective control point for two-way fluxes between the root and the soil[15]. Together, the endodermis and the exodermis coordinate their critical roles in regulating the two-way fluxes of water, solutes and gases and protecting plants against environmental stressors, and they each

integrate numerous environmental cues into their differentiation programs to optimize their functions.

While the endodermis is one of the best characterized plant cell types for their development and differentiation[16,17], the exodermis remains relatively unexplored because the model for root development, *Arabidopsis thaliana*, lacks the cell type[18]. However, the exodermis in its diverse morphologies is found in around 90% of flowering plants[19–21]. Considering the ABA-induced differentiation program in endodermis and exodermis, there is diversity also in its regulation across the flowering plants but universally, the SL deposition program is regulated by a group of closely related MYB (MYELOBLASTOSIS) transcription factors (TFs)[22,23]. In Arabidopsis, ABA induces the deposition of endodermal SL via multiple, redundantly acting MYBs from clades S10, S11 and S24[24,25] including AtMYB39, AtMYB41, AtMYB53, AtMYB92 and AtMYB93[2,26,27]. Similarly in rice, four MYBs, OsMYB39a, OsMYB41, OsMYB92a, and OsMYB92b, were identified as the redundant core regulators of endodermal SL, which also were responsive to ABA[4]. Intriguingly, these rice MYB TFs do not affect the exodermal SL which also are deposited in rice roots in response to ABA, suggesting that a separate set of TFs is required for exodermal SL in rice. In contrast, tomato has SL only in the exodermis and the homologs of these MYBs, specifically SlMYB92, SlMYB41 and SlMYB63, regulate the exodermal SL in a non-redundant fashion[3,28]. So, a set of conserved MYBs are seen to regulate the SL differentiation program, which is active in an ABA-responsive fashion in either endodermis or exodermis depending on the angiosperm species. However, the direct link between ABA signaling and this cell-type-specific differentiation program coordinated by the MYBs has remained unknown.

Exodermis has been reported to be found in the majority of angiosperm families, with only a small number of families having species either with and without an exodermis[19–21,29]. Legumes (Fabaceae) were originally reported as one of the clades not containing species with an exodermis[19] and it was hypothesized that the presence of a barrier at the outermost cortex layer would be inhibitory to the legumes' ability to form symbioses with nitrogen-fixing bacteria in root nodules formed from the cortex layer[30]. In the past two decades there has been contrasting reports of the presence of exodermis in different legumes such as pea (*Lathyrus oleraceus*, previously *Pisum sativum*)[19,31,32] and chickpea (*Cicer arietinum)*[33,34], and this may be due to the stress-induced, dynamic nature of the exodermis in many species. Intrigued by this gap of knowledge and potential diversity of root barriers in legumes, we set out to characterize the ABA-responsive differentiation programs in a selection of galegoid legumes.

Results

To investigate the effect of ABA on root suberization, we grew eight species from the galegoid family in the presence or absence of 2μM ABA (Figure 1A). After 3 days, root cross-sections were stained with Fluorol Yellow (FY) and Basic Fuchsin (BF), fluorescent dyes that bind to suberin and lignin, respectively[35–38], and the fluorescence intensity was quantified across individual cell layers (Figure 1B). ABA induced suberization and lignification in distinct root cell layers across the galegoid clade (Figure 1C, S1). In chickpea and *L. oleraceus*, ABA promoted suberin accumulation specifically in the outermost cortical cell layer (C1) and not in the endodermis (EN). In contrast, ABA induced the suberization of the endodermis in *Lens culinaris* (lentil), *Medicago truncatula* (barrel medic), *Medicago sativa* (alfalfa), and *Trifolium repens* (white clover), with a weak FY signal observed in cortical cell layers. *Vicia sativa* (common vetch) displayed a unique pattern of suberization in multiple outer layers of the root cortex as well as in the endodermis in response to ABA. In *Lotus japonicus* (narrowleaf trefoil), the process of root suberization in the endodermis occurred independently of ABA at the sampled developmental stage, and indeed developmental stage affected the number of suberized cells (Figure S2). Suberin monomer profiling further confirmed that ABA promotes the accumulation of suberin monomers in chickpea, *M. truncatula*, and *V. sativa* (Figure 2A,B), with the overall increase of *cis*-

and *trans*-ferulic acid, long-chain fatty acids (C18, C20, C22), α-ω-diacids (C16, C18:1, C18) and ω-hydroxy acids (C22) (Figure S3).

Given these diverse patterns of suberin accumulation, we examined the ultrastructure of the suberin in C1 layer (Figure 2C) and endodermis (Figure S4) using transmission electron microscopy (TEM) for three species with contrasting FY phenotypes. In chickpea roots grown in the presence of ABA, C1 displayed a clear suberin lamella (SL), characterized by a pattern of alternating dark and light bands[39] (Figure 2C). In contrast, while the SL was clearly present in the endodermal cell layer of *M. truncatula* and *V. sativa* (Figure S4), it was absent in the C1 cells in these species (Figure 2C). Despite the high FY signal detected in the cortex of *V. sativa* (Figure 1C), TEM revealed an amorphous suberin structure lacking the alternating banding pattern typical for SL.

To determine if ABA-induced compounds in the cortex of these species function as an apoplastic diffusion barrier, we tested if they restrict the diffusion of propidium iodide (PI)[7,8]. PI apoplastic diffusion was blocked in chickpea roots treated with ABA as indicated by the lack of PI fluorescent signal in inner cortical cell layers when compared to mock-treated roots (Figure 2D). This suggests that ABA-induced cell-type-specific modifications in the cell wall of C1 results in the establishment of a functional apoplastic barrier in chickpea. This supports the chickpea C1 being a functional exodermis. However, this cannot be attributed solely to the accumulation of suberin, as lignin, the main component of the Casparian strip and critical for blocking apoplastic diffusion[8,14], was also present (Figure S1). In *M. truncatula* and *V. sativa*, PI diffused into the inner cortex layers in both mock and ABA-treated roots (Figure 2D). The cortex layers with FY and BF signal also resulted in strong PI signal in chickpea and *V. sativa* (Figures 1C and 2D), which may relate to cross-reactiveness of PI with the cell wall modifications. In summary, our results demonstrate that the stress hormone ABA promotes suberin and lignin accumulation in the outer cortex of various legume species. Specifically, chickpea exhibited a robust single-layer response with deposition of structured suberin lamellae (SL) and lignin and forming a functional apoplastic diffusion barrier.

The suberin biosynthesis and deposition pathway is a coordinated process with many enzymes that operate in different cellular compartments[40] (Figure 3A). To understand how the process of ABA-induced exodermal differentiation leading to apoplastic barrier formation is transcriptionally regulated, we profiled the chickpea root transcriptome at nine different timepoints: 15, 30 and 45 minutes, and 1 h, 2h, 4h, 6h, 8h and 24h after mock or ABA exposure (Figure 3A). ABA induced primarily upregulation of gene expression (Figure 3B). K-means clustering of differentially expressed genes (DEGs) identified temporal expression patterns in response to ABA (Figure 3C). Genes exhibiting a rapid upregulation (30 to 45 minutes) were grouped into Cluster I, while Clusters II, III, and IV represented delayed transcriptional responses, with upregulation of genes at 2h, 4h and 6h, respectively (Figure 3C-E). Genes involved with the general ABA response, like orthologues to the Arabidopsis *ABA INSENSITIVE1* (*CaABI1*: *Ca_05930*), *HIGHLY ABA-INDUCED PP2C GENE3* (*CaHAI3: Ca_13069* and *Ca_15032*), *RESPONSIVE TO DESICCATION 29B* (*CaRDB29B*: *Ca_04473*), LATE EMBRYOGENESIS ABUNDANT 4-5 (CaLEA4-5: *Ca_07309*, *Ca_14189* and *Ca_21274*) and ABA-responsive Kinase (*CaPKINASE*: *Ca_04411*) to be mainly found in Cluster I (Figure 3E-F, S5). In contrast, suberin biosynthesis genes, like *GLYCEROL-3-PHOSPHATE SN-2-ACYLTRANSFERASE1, 5, 6* and *8* (*CaGPAT1*: *Ca_15259*, *CaGPAT5*: *Ca_16115*, *CaGPAT6*: *Ca_25903* and *CaGPAT8*: *Ca_13742*) *LACCASE3* and *5* (*CaLACS3*: *Ca_17272* and *CaLACS5*: *Ca_12445*), *ALIPHATIC SUBERIN FERULOYL-TRANSFERASE* (*CaASFT*: *Ca_26067*) and GDSL-type/lipase (GELP) enzymes (*CaGELP*: *Ca_00361*, *Ca_06369*, *Ca_09232* and *Ca_24203*) were found in Clusters II, III and IV (Figure 3E,G, S5). Matching the transcriptional timing, suberin accumulation in C1 could be detected by FY after 24h (Figure S6). In summary, the expression of suberin biosynthesis genes is temporally separated from genes in the general ABA response in chickpea roots.

To understand the transcriptional regulatory mechanisms underlying the temporal separation between ABA general response and the suberin biosynthesis program, we analysed the DNA *cis*-element composition of promoters of cluster I, II, III and IV genes (Figure 4A,B, S7). Motif enrichment analysis revealed that the GBOX *cis*-element (CACGTG), the main DNA element targeted by the canonical ABA response[41,42] was significantly enriched in the promoters of cluster I, but not in the promoters of cluster II, III and IV (Figure 4A, S7). This confirms that the rapid transcriptional response observed in chickpea roots occurs through the canonical ABA signalling pathway[43]. We observed other *cis*-elements enriched in the promoters of cluster II and II, including that of suberin-regulating MYB TFs (ACCTA)[22,44,45] (Figure 4B, S7). Additionally, other DNA elements were found to be enriched in the promoters of the delayed ABA response, like WRKY40 (TTGACT) and NF-YA (CCAAT) binding *cis*-elements (Figure S7). This indicates that albeit ABA-induced, suberin biosynthesis in the chickpea exodermis is not directly controlled by the canonical ABA signalling pathway. Instead, it appears to be regulated through ABA-induced changes in the regulatory state of exodermal cells, with the involvement of other TFs, like MYBs, that control the temporally separated expression of suberin biosynthesis genes.

Based on these results, we hypothesize that ABA mediates changes in the regulatory state of chickpea root cells by enhancing the expression and/or activity of specific MYB TFs through the canonical ABA signalling pathway. These MYB TFs, in turn, initiate the gene regulatory networks to activate MYB TFs directly associated with the suberin biosynthesis program in chickpea roots. Among the ABA-induced *MYBs*, *Ca_00232* and *Ca_14119* were rapidly upregulated within 45 minutes of ABA exposure (Figure 4E). Phylogenetic analysis revealed that *Ca_00232* shares a close evolutionary relationship with *AtMYB74* and *AtMYB102*, while *Ca_14119* is closely related to *AtMYB41*(Figure S8). In Arabidopsis, these MYB TFs were characterized as direct targets of the ABA signalling, and AtMYB41 regulates the suberization of the root endodermis[1,2,26,46,47]. Other MYBs presented a delayed response to ABA in a similar temporal pattern as the expression of suberin biosynthesis genes (Figure 4E, S5). For instance, *Ca_11228*, *Ca_11494* and *Ca_11832*, close orthologues of the Arabidopsis *SUBERMAN* (*AtMYB39*) (Figure S8), was upregulated at 4 h and 24 h by ABA (Figure 4E). The Arabidopsis the SUBERMAN TF was able transactivate the promoters of suberin biosynthesis genes[27].

We hypothesized *Ca_00232* to be a direct target of the canonical ABA signalling pathway as its promoter contains two GBOX elements. We conducted transient assays in Arabidopsis leaf protoplasts to evaluate if ABA is sufficient to induce the activation of the *Ca_00232* promoter (Figure 4F). We cloned the promoters of *Ca_00232*, *Ca_11228* (a *MYB* with a delayed response to ABA) and *Ca_04411* (quick response to ABA) to drive the firefly luciferase gene in a dual luciferase assay (Figure 4F). We transfected the constructs into Arabidopsis leaf protoplasts which were then treated with ABA (10 µM) or mock for 3 h. The promoters of *Ca_04411* and *Ca_00232*, but not *Ca_11228* were transcriptionally active in response to ABA (Figure 4F). These results support our hypothesis that *Ca_00232* is a direct target of the canonical ABA signalling pathway, potentially connecting ABA perception and suberin biosynthesis in chickpea.

Because suberin deposition in response to ABA is highly cell-type-specific in chickpea roots, we profiled the transcriptome of over 10,000 protoplasts isolated from ABA-treated roots (Figure 5A). We detected 8,639 high-quality cells in our dataset which formed 22 UMAP clusters with representative marker genes (Figure 5B). To be considered a marker gene, a gene should have expression in at least 20% of cells of the marked cluster, a percentage difference of at least 20% to other clusters, an average logFC greater than 1, and an adjusted P-value lower than 0.01 (Figure 5C). Identical clusters and markers were observed in the replicate experiment (Figure S9). To identify the identity of the clusters, we compared if orthologues of marker genes were characterized as marker genes in the *Arabidopsis* scRNA-seq root database scPlantDB (Figure S10)[48]. For instance, the meristematic cell and the endodermis cortex initials (ECi) clusters showed high similarities to cell division markers clusters in the scPlantDB (meristematic cell, G1/G0 phase, G2/M phase and S phase) (Figure 5C, S10A). Half of our xylem cell cluster marker

genes had an orthologue annotated as a marker for xylem (47%) or metaxylem (56%) clusters in Arabidopsis, (Figure S10B). We further analysed the expression of empirically determined root cell markers in Arabidopsis[49] to refine the annotation of individual clusters, including cortex, phloem and epidermis (Figure S11). Altogether, this approach allowed us to identify the cell types that the 22 UMAP cluster likely correspond to (Figure 5B).

In accordance with what we observed at the cellular level (Figure 5D,E), our single cell transcriptome data revealed a spatial separation between the regulatory programs for Casparian strip development in endodermis and suberization in exodermis (Figure 5F). The orthologs of the genes involved in Casparian strip formation were exclusively expressed in the endodermal cluster (Figure 5F), including *GASSHO1/SCHENGEN3* (*GSO1/SGN3*), *CASPARIAN STRIP MEMBRANE PROTEINs* (*CASPs*) and their regulator MYB36[9,50,51]. Additionally, the Casparian strip formation in Arabidopsis requires the stele-produced peptide CASPARIAN STRIP INTEGRITY FACTOR1 (CIF1)[12,13]. We observed that also in chickpea, the closest orthologue to *AtCIF1* (*Ca_20263*) was highly expressed in stele cell clusters (Pericycle 1 to 3, Phloem1 and Stele Initials). Then, to identify the exodermis cells that do not exist in Arabidopsis, we used the expression of suberin biosynthesis genes (Figure 5E). Among them, we identified one *CaASFT1* (*Ca_26067*), *CaLAC5* (*Ca_12445*), two *CYP86s* (*CaCYP86A1*: *Ca_15610*; *CaCYB86B1*: *Ca_11097*), two *KCSs* (*CaKCS1*: *Ca_01346*; *CaKCS11*: *Ca_12147*); one *ABCG* (*CaABCG23*: *Ca_21808*), four *GPATs* (*CaGPAT1*: *Ca_15259, CaGPAT5*: *Ca_16115, CaGPAT6*: *Ca_25903* and *CaGPAT8*: *Ca_13742*) and two *GELPs* (*CaGELPa*: *Ca_09232*; *CaGELPb*: *Ca_24203*) to be mainly expressed in the exodermis cluster (Figure 5F). Overall, these annotated cell clusters provide an atlas of cell types of the chickpea root and offer valuable insights into the molecular mechanisms of root cell-type-specific responses to ABA.

After the successful annotation of these clusters, we queried the spatial expression of the ABA-induced *MYBs* identified in the time-course experiment (Figure 4E). Interestingly, *Ca_00232*, was significantly expressed in the exodermis cluster, but also in root cap (Rootcap 2, 3 and 4) and epidermis clusters (Trichoblast_1) (Figure 5F). A similar pattern was observed for the other two *MYBs Ca_14119* and *Ca_17479* (Figure 5F), while Ca_*11228* expression was restricted solely in the exodermis cluster (Figure 5F). Rest of the ABA-induced *MYBs* were found to be lowly expressed in the exodermis or expressed primarily other cell types. For instance, *Ca_07872*, was primarily expressed in the Pericycle clusters (Pericycle 1 to 3), while *Ca_11494*, *Ca_11832*, *Ca_08170* and *Ca_06925* were lowly expressed in the exodermis or not detected in our single-cell data (Figure 4F). Altogether, these data suggest that ABA can promote the expression of MYBs TFs in a cell-type-specific manner in the chickpea root. However, since we observed that many of the suberin biosynthesis genes to be solely expressed in the exodermis, we propose that exodermis is uniquely specialized to translate the ABA-mediated changes in the regulatory landscape into the activation of the suberin biosynthesis program. In accordance with this, we observed that genes previously identified as part of the fast general ABA response (Cluster I, Figure 3D) had a scattered response throughout the different cell clusters of the chickpea root (Figure S12, S13) while the genes involved with the delayed response, particularly genes in Cluster II and IV were primarily expressed in the exodermis cluster (Figure S12).

To reconstruct the spatial and temporal dynamics of ABA-induced suberization in the exodermis, we utilized the Slingshot package[52] to map developmental trajectories of outer cortex and exodermis cells (Figure 6A). Unsupervised lineage detection revealed two main lineages starting from the Meristem_1 cluster, lineage 1 to Exodermis_1 and lineage 2 to OuterCortex_2, both *via* OuterCortex_1 (Figure 6A&B). Pseudotime estimation in lineage 1 revealed that the expression of suberin biosynthesis genes initiate late in the exodermal developmental trajectory (Figure 6C). This reflects the ABA-induced temporal expression changes combined with the developmental trajectory along the root in chickpea (Figure S2). When looking at the expression of *MYBs* along the pseudotime trajectory, we observed that the majority of *MYBs* upregulated by ABA showed expression patterns similar to the suberin biosynthesis genes (Figure 6D). However, similarly to

the time-course data (Figure 4E), *Ca_00232* showed an early expression pattern along the exodermal lineage trajectory (Figure 6D). Thus, our single-cell analysis further reiterates the potential role of *Ca_00232* as the transcriptional link between the early ABA perception and the delayed spatial control of suberin biosynthesis in the chickpea root exodermis.

Our characterization of ABA-induced differentiation trajectories of galegoid legume cortical layer uncovered diversity in their ability to deposit cell wall polymers that form functional apoplastic barriers. Transcriptional investigation of the chickpea exodermis differentiation trajectories with time-course and single cell approaches revealed a group of putative MYB TFs that connect general ABA signaling into exodermis-specific differentiation (Figure 6E).

Materials & methods

Sterilization and germination of legume seeds

Legume seeds were obtained from the following sources: *C. arietinum* Anigiri accession ICC 5679 from ICRISAT; *L. oleraceus* Cameor[53] from Judith Boursin, *L. culinaris* Groene Dupuis and *V. sativa* Prontivesa from Vreeken's Zaden (the Netherlands), *L. japonicus* Gifu from Tonni Andresen, *M. truncatula* A17 from Wouter Kohlen, and *M. sativa* and *T. repens* from Intratuin B.V. (the Netherlands).

Seeds from *C. arietinum* Anigiri, *L. oleraceus* Cameor, *L. culinaris* Groene Dupuis, *V. sativa* Prontivesa, *T. repens,* and *M. sativa* were gas sterilized by placing the seeds in a desiccator with a mixture of 50 mL of commercial bleach and 2.5 mL of HCl for 24 hours. After sterilization, seeds were soaked in distilled water for 12 hours in the dark at room temperature. Soaked seeds were placed onto sterile 0.7% (w/v) Phytoagar (Duchefa) dissolved in water. Seeds were then germinated in the dark for 3 days at 25°C. For the germination, plates were kept in a 60° to 70° angle to ensure a uniform growth direction of the roots. For *M. truncatula* A17, seeds were scarified for 7 minutes using sulfuric acid and sterilized for 7 minutes with 10 % (v/v) commercial bleach. After sterilization, the seeds were washed five times with distilled water and kept in water for 12 hours. After soaking, seeds were placed on petri dishes containing 1% (w/v) Phytoagar and cold stratified in the dark at 4°C for three days. To initiate germination, the petri dishes were inverted horizontally (with the medium on top) and transferred to growth cabinets at 25°C in the dark for 12 hours. Germinated seedlings were then transferred to 0.7% (w/v) Phytoagar plates and kept in the dark for another 36 hours in a 60° to 70° standing angle. For *L. japonicus* Gifu, seeds were mechanically scarified with sandpaper and surface sterilized with 10% commercial bleach for 10 minutes. After sterilization, seeds were washed five times and soaked in water at room temperature for 12 hours. Seeds were then transferred to plates with 1% (w/v) Phytoagar and cold-stratified at 4°C in darkness for 3 days. Seeds were germinated at 25°C in darkness for five days and plates were placed in 60-70° angle.

Suberin and lignin histology and fluorescent signal quantification

Four-day old seedlings of, *C. arietinum* Anigiri, *P. sativum* Cameor, *L. culinaris* Groene Dupuis, *V. sativa* Prontivesa, *T. repens* and *M. sativa*, two-day old seedlings from *M. truncatula* A17, and five-day old seedlings from *L. japonicus* Gifu were transferred to ½ MS square plates supplemented with 2 µM ABA or mock conditions. The seedlings were maintained in a D-root system[54] in growth chamber under long-day conditions (16 h light, 8 h dark; 25°C; 70% humidity). After 3 days, 1-cm root segments at the middle point of the root (50% region) were vacuum-infiltrated for 1 h in a solution containing 4% (w/v) paraformaldehyde (PFA) dissolved in PBS buffer. After vacuum infiltration, roots were kept in 4% PFA for at least 12 hours at 4°C and subsequently washed three times with PBS. Root segments were embedded in 4% (w/v) agarose (*C. arietinum*, *P. sativum*, *L. culinaris*, *V. sativa*) or 3% (*M. truncatula*, *M. sativa*, *L. japonicus*, *T. repens*) and cross-sectioned into 250 µm thick sections using the VT 1000 S vibratome (Leica). Fluorescent staining and

confocal imaging of suberin and lignin in root cross sections was performed as described previously[28]. The quantification of FY and BF fluorescent signals along individual cell layers of the root were done using the Icy software (https://icy.bioimageanalysis.org/). To analyse fluorescence intensity, 2D polylines were manually traced along the anticlinal cell walls of at least 10 individual cells from different cell layers within each root cross-section. The 'Path Intensity Profile' plugin in Icy was used to measure the maximum pixel intensity for each cell wall in the FY or BF channels. For background correction, random points along the root surface were selected to estimate the overall background signal for each image. The average background signal of each image was subtracted from the maximum pixel intensity of each cell wall. Finally, for each image, the fluorescence signal of the cell layer was determined as average signal intensity across all measured cells of the layer. Quantification was done using cross-sections of at least 8 individual roots in mock or ABA conditions and statistical differences were determined based on Wilcoxon rank-sum test with a Benjamini-Hochberg adjusted P-value threshold of 0.05 was used to indicate the statistical significance.

GC-MS

For the profiling of suberin monomers, four-day-old seedlings of *C. arietinum* Anigiri and *V. sativa* Prontivesa and two-day-old seedlings of *M. truncatula* A17, were transferred to magenta boxes filled with sterile ½ MS medium supplemented with or without 2 µM ABA. A metal grid was placed in the magenta boxes to ensure that only the root was in direct contact with the liquid medium. The seedlings were maintained in the magenta boxes under long-day conditions (16 h light, 8 h dark; 25°C; 70% humidity), under slow agitation (20 rpm) for 24 hours. Root samples (root tip to the 50% region of the root) were collected for an average of 350, 210 and 50 mgs of fresh weight (FW) tissue per biological replicate for *C. arietinum, V. sativa and M. truncatula*, respectively. Root samples were immediately placed in hot isopropanol (70°C) for 30 minutes. Root samples were extracted using a Soxhlet apparatus for 8 hours, first with chloroform followed by methanol, to eliminate all soluble lipids. Subsequently, extracted tissues were dried over silica gel in a desiccator. Suberin monomers were released through transesterification with boron trifluoride in methanol at 70 °C overnight. Dotriacontane (0.2 µg/µl) was added to each sample as an internal standard. Saturated sodium bicarbonate was added to stop the transesterification reaction, and the fraction of suberin monomers were extracted using chloroform. The chloroform extract was washed with water, and residual water was with sodium sulfate. The chloroform fraction was then reduced to a final volume of approximately 50 µL and derivatized with N,N-bis(trimethylsilyl)trifluoroacetamide (BSTFA) and pyridine at 70 °C for 40 minutes. Gas chromatography (GC) equipped with a flame ionization detector (6890 N Network GC System, Agilent Technologies) was used to separate and quantify the compounds. For compound identification, gas chromatography coupled with a mass spectrometry selective detector (GC-MS; 5977A MSD, Agilent Technologies) was utilized and fragmentation spectra were matched against an internal library of known suberin monomers and the NIST database for identification.

Transmission Electron Microscopy (TEM)

Germinated seedlings of chickpea, *M. truncatula* and *V. sativa* were transferred for 3 days on plates with either mock or 2 µM ABA treatment. After three days on treatment 1 cm root pieces were harvested in the 75% region of the individual roots. Root pieces were fixed in 2.5% glutaraldehyde + 2% paraformaldehyde in phosphate buffer (PB 0.1M) at 4°C for at least two weeks. After incubation, samples were washed 6 times for 10 min in PB, incubated in 1% osmium tetroxide dissolved in PB for 1 h, and washed again 3 times for 10 min using MiliQ water. Samples were dehydrated using concentration gradient of acetone solutions (10% for 15 min, 30% for 15 min, 50% for 15min, 70% for 15 min, 80% for 15min, 90% for 15 min, 96% for 10 min, 100% for 15 min, 100% for 30 min). This was followed by infiltration with LR white in a concentration gradient (1:2 LR white: EtOH for 1 h, 1:1 LR: EtoH for 1 h, 2:1 LR white: EtOH for 1 h, 100% LR white for 2 h,

100% LR white overnight at room temp, 100% resin for 2 h) and polymerized for 24 h in an oven at 60-65°C. Polymerized samples were cross-sectioned to 50 nm thickness for *M. truncatula* and chickpea, and *V. sativa* was sectioned to 70 nm thickness using a Leica ultramicrotome UC7, before attaching to 100 mesh carbon grids. The grids were incubated for 10 min using 2% uranyl acetate followed by 5 washes with MiliQ water. Next, the grids were incubated with lead citrate (EMS) for 10 min in a CO_2-free environment. The grids were washed two times with 0.01 N CO_2-free water followed by 3 final washes with MiliQ water. Sample preparation, processing and imaging were carried out by the Wageningen Electron Microscopy Centre. A JEOL JEM1400 transmission electron microscope was used to image the samples.

Propidium iodide diffusion assay

Four-day-old seedlings of *C. arietinum* Anigiri and *V. sativa* Prontivesa and two-day-old seedlings of *M. truncatula* A17, were transferred to new ½ MS square plates supplemented with 2 µM ABA or mock conditions. The seedlings were maintained in a D-root system[54] in growth chamber under long-day conditions (16 h light, 8 h dark; 25°C; 70% humidity). After 3 days, root segments up to the 75% region, including the root tip, were exposed to 30 µg/mL propidium iodide solution in the dark at 28 °C for 2 hours. Root segments were washed twice in MilliQ water and 0.5 cm segments from the 50% region of the root were excised and embedded in 4% (w/v) agarose for C. arietinum and V. sativa and in 3% (w/v) agarose for *M. truncatula*. Root cross-sections (250 µm thick) were obtained using the VT 1000 S vibratome (Leica). Confocal laser scanning microscopy was performed on a Zeiss apotome microscope with the ×20 objective at 405 nm excitation and 600–650 nm detection. The quantification of the cell-layer PI intensity was done as described above.

RNAseq harvest, libraries, sequencing

Four-day-old seedlings of *C. arietinum* Anigiri were transferred to magenta boxes filled with sterile ½ MS medium supplemented with or without 2 µM ABA. Like the GC-MS experiments, chickpea seedlings were placed on top of a metal to ensure that only the root was in direct contact with the liquid medium. Seedlings were maintained in the magenta boxes under long-day conditions (16 h light, 8 h dark; 25°C; 70% humidity), under slow agitation (20 rpm) until the time of harvest. Lower 50% of the roots from the mock and ABA treatments were harvested at nine different timepoints: 15, 30 and 45 minutes, and 1 hour (h), 2h, 4h, 6h, 8h and 24h after ABA exposure. Three roots were sampled for each individual biological replicate. Samples were collected in 2-ml tubes containing ceramic beads and ground using a tissuelyser (Retsch MM300). The mRNA extraction and library preparation were performed according to the non-strand specific random primer-primed RNAseq library protocol of Townsley et al. (2015). The libraries were pair-end sequenced (150 bp) using NovaSeq X Plus.

RNAseq mapping, data analysis

We quality trimmed paired-end reads using Trim Galore (version 0.6.6) [55] using default settings. After trimming, reads were pseudo-aligned to the CDC Frontier chickpea reference transcriptome (Phytozome, https://phytozome-next.jgi.doe.gov/) using Kallisto (version 0.46.2) [56] with the following parameters: -b 100. DEGs were identified using the R package limma[57] according to Jo et al. (2024). For every time point, we compared the ABA and mock treated samples using edgeR[58] and DEG were determined as genes with an Benjamini-Hochberg adjusted P value < 0.05 and at least 2-fold changes between treatments. DEGs were clustered based on their logFC values across all time points using kmeans function from R (k=8). Annotation of DEGs was based on annotation info for the CDC Frontier genome on Phytozome.

Promoter motif enrichment analysis

DNA motif enrichment analysis was performed as described[59], using the DNA motifs: GBOX (CACGTG), MYB (ACCTA), ATHB7 (ATNATTG), bHLH122 (CNACTTG), NF-YA (CCAAT), ANAC058 (CNTNNNNNNNANG), WRKY40 (TTGACT) and HAT5 (AATAATT) to screen the promoter regions

(500 bps upstream the ATG) of DEGs identified in clusters I, II, III and IV. In summary, motifs were screened for enrichment using HOMER (homer.ucsd.edu/homer/motif/index.html) using the known function. For each DEG cluster, we generated 1000 sets of randomly selected genes that were of comparable number. Each set of promoters from each cluster were compared against the promoters of the respective 1,000 sets of random genes to calculate the P value significance of enrichment. P values were adjusted using the Bonferroni method, and a significance threshold of $P < 0.01$ was used to identify significantly enriched DNA motifs.

Phylogenetic tree construction

Phylogenetic trees were generated using the methods described in Jo et al. 2024. In summary, Full length amino acid sequences of chickpea upregulated MYBs and all annotated Arabidopsis MYB TFs were aligned using MAFFT (https://mafft.cbrc.jp/alignment/server/). The phylogenetic tree was determined using the maximum likelihood method with 1000 bootstraps using iQ-TREE (http://iqtree.cibiv.univie.ac.at/).

Cloning of promoters for transient assays

Promoters (500 bps upstream the start codon) of *CaPKINASE* (*Ca_04411*), *CaMYB74/102* (*Ca_00232*) and *CaMYB39* (Ca_*11228*) were PCR amplified from the *C. arietinum* Anigiri genomic DNA and cloned into the dual luciferase vector (pDLUC15) as described previously[28].

Transient Expression Assays in Arabidopsis leaf protoplasts

Transient assays of firefly and Renilla luciferase activity in protoplasts were performed as described previously[28]. After transfection, protoplasts were incubated in mock or ABA (10 µM) conditions for 3 hours, and firefly and renilla luciferase activity was assessed as described in Jo et al. 2024. All trials were done with at least three biological replicates, and student t test with a significance P value threshold of 0.05 was used for the statistical analysis.

Chickpea root protoplast isolation and scRNA-seq

For the scRNA-seq analysis we used protoplasts from roots (3 cm above the root tip) of 3-day old chickpea seedlings grown in the presence of 2 µM ABA for 24 h. Approximately 15 roots were collected, cut into 1-2 mm slices and vacuum infiltrated for 15 minutes immersed in an enzyme solution consisting of 0.4 M D-Sorbitol, 20 mM KCl, 20 mM MES, 10 mM CaCl2, 0.1% (w/v) BSA, 1.5% (w/v) Cellulase R10 (Duchefa), 0.5% (w/v) Macerozyme R10 (Duchefa), 5% (v/v) Viscozyme® L (Sigma) and 3.56 mM of 2-Mercaptoethanol. Roots were kept in the enzyme solution for 2 h under 40 rpm, and the resulting protoplast solution was filtered through a 40 µm mesh and centrifuged for 5 min at 200 x g at 4°C in a swinging bucket centrifuge with the de-acceleration set to minimal. Protoplasts were resuspended in 2 mL of resuspension solution (0.4 M D-Sorbitol, 20 mM KCl, 20 mM MES, 1 mM CaCl2, 0.1% (w/v) BSA, 3.56 mM of 2-Mercaptoethanol). Chickpea root protoplasts were purified using a three-phase density gradient using Optiprep™ (Stemcell™ Technologies). An Optiprep™ working solution (WS) was prepared by mixing 0.06g of KCl into 10 mL of Optiprep™. The density gradient was prepared in a 5 mL tube as follows: In the bottom layer, 2 mL of protoplast cell suspension was gently mixed and homogenized with 500 µL of OptiPrep™ WS (final density: 1.064 g/mL). For the middle layer, 1 mL of a mixture of 2 mL of resuspension buffer with 400 of OptiPrep™ WS(final density: 1.053 g/mL) was gently pipetted at the top of the bottom layer. For the topmost layer, 200 µL of the resuspension solution was carefully pipetted on top of the middle layer. The prepared gradient was centrifuged at 200 x g at 4°C for 5 minutes using a swinging bucket centrifuge. Following centrifugation, the protoplasts, concentrated in the topmost layer, were carefully collected, centrifuged again for 5 min at 200 × g at 4°C and resuspended to a final concentration of ~1,000 cells per µl in resuspension solution. The protoplast suspension was loaded into microfluidic chips (10X Genomics) and subsequently processed using the 10x Chromium Controller from 10x Genomics, Single-cell libraries were

constructed using the Single Cell 3' v3.1 Kit (10x Genomics) following manufacturer instructions. Sequencing was performed using NovaSeq X Plus (PE150).

Single-cell transcriptome analysis

Reads were mapped using cellranger (10X Genomics) to the CDC Frontier chickpea reference genome (Phytozome, https://phytozome-next.jgi.doe.gov/) with appended chloroplast genome of chickpea (NC_011163.1) and the mitochondrial genome of *M. truncatula* (NC_029641.1). For an improved alignment, a modified version of the current Carietinum_492_v1.0 (Phytozome) was used. Due to the 3' bias of sequencing reads generated by the 10X Single Cell 3' v3.1 library kit, the 3' UTR regions of all genes in the chickpea genome were expanded by 500 bps using BEDTools[60], as the Carietinum_492_v1.0 gene model lacks annotated 3' UTR regions. Before analysis in Seurat[61], the fraction of background reads was removed using SoupX[62], cell doublets were removed using scDblFinder[63], and low-quality cells were identified and removed based the number of detected features (< 800 features) and mitochondrial and chloroplast gene counts (> 5% of mitochondrial and chloroplast counts), which resulted in the detection of 8,639 high-quality cells. Uniform manifold approximation and projection (UMAP) were calculated using 50 principal component dimensions and cell-clusters were identified using the Seurat 'FindClusters' function with the resolution parameter set to 0.8. Markers for each UMAP cluster were identified using the using the Seurat 'FindAllMarkers' and filtered for an average log2FC greater or equal than 1, adjusted P values lower or equal 0.01, percentage of cells within the cluster that expresses the gene greater than 20% and percentage difference to other clusters greater than 20%. The identities of specific UMAP clusters were annotated by comparing whether orthologues of marker genes were characterized as marker genes in the Arabidopsis scRNA-seq root database (scPlantDB)[48] and those empirically determined from the Arabidopsis scRNA-seq root atlas[49]. Additionally, the exodermis and endodermis cell clusters were identified based on the expression of a manually curated list of suberin biosynthesis genes and Casparian strip genes, respectively.

Lineage detection and pseudotime trajectory analysis

Lineage detection and pseudotime trajectory was performed using the cell clusters representing the outer ground tissue (outer cortex 1 & 2 and exodermis). The meristem_1 cluster was included to anchor the cell lineage detection and pseudotime estimations. Lineage detection and pseudotime trajectory were detected using the Slingshot R package[52] with the 'getLineages' and 'slingshot' functions, respectively.

Data availability

All sequencing data will be openly released upon acceptance of the manuscript for publication.

Acknowledgements

We would like to thank Judith Boursin for pea seeds, Wouter Kohlen for *Medicago truncatula* seeds and extensive conversations, and Tonni Andresen for *Lotus japonicus* seeds and support. We also thank Xiren Cao, Henri Essombé Kuoh and Menno Druif for technical assistance, and the WUR TEM facility for imaging.

Author contributions

KK: Conceptualization, Supervision, Project Administration, Funding Acquisition.
LJ, RK, SB, JH, HC: Investigation.
RBF, PD: Resources.
LJ: Data Curation, Formal Analysis.
LJ, RK: Visualization.

LJ, KK: Original Draft.
All authors: Writing – Review & Editing.

Conflict of interest

No conflict of interest declared.

Funding statement

This work was supported by Netherlands Organization for Scientific Research (NWO) VIDI grant number VI.Vidi.193.104 to KK.

Figure Legends

Figure 1. Galegoid legumes deposit suberin to the cell walls of different root cell types in response to ABA. a, Representative phylogenetic tree of the galegoid legume clade. The tree was adapted from[64]. Species marked with an arrow correspond to species used in this study. *Lens culinaris* is nested in the genus *Vicia*[65]. **b,** Graphical representation of the survey for observing cell-type suberization in legume roots treated with mock or ABA (2 µM) for 3 days. The middle point of the root (50%) was cross-sectioned, stained with FY and counter-stained with aniline blue. Finally, the fluorescence levels of cell walls of individual cell layers of the root epidermis (EP), the four outermost cell layers of the cortex (C1 to C4), the endodermis (EN) and the pericycle (PE) were quantified. **c,** Quantification summary of FY intensity across multiple cell layers of legume roots in response to ABA. For each species, the top images show representative confocal images of cross-section of roots treated with mock or ABA, with the FY signal overlaid on top of bright field images (scale = 25 µm). The yellow and green arrow depicts the position of the outermost layer of the cortex and endodermis, respectively. On the bottom, the heatmaps show the average pixel intensity of the FY signal in different layers of the root cross section. Asterisks indicate significance based on Wilcoxon rank-sum test with a Benjamini-Hochberg adjusted P-value. Threshold of 0.05 was used to indicate the statistical significance ($n \geq 8$).

Figure 2. Biochemical, structural and functional evaluation of ABA-induced cell wall modifications show that chickpea forms an exodermis with a suberin lamella and an apoplastic diffusion barrier. a, Principal Component Analysis (PCA) of suberin monomer abundances in roots of chickpea, *M. truncatula* and *V. sativa* treated with mock or 2 µM ABA for 24 hours. **b,** Abundance of major classes of suberin monomers in roots treated with mock (grey) or 2 µM ABA (red) for 24 hours. Asterisks indicate significance based on Student's t-test with a P-value threshold of 0.05 ($n = 4$). **c,** Transmission electron microscopy (TEM) cross-sections at the 50% region of Chickpea, *M. truncatula* and *V. sativa* roots treated with mock or 2 µM ABA for 3 days. The cell wall (CW) depicted in the images refers to the cell wall between two adjacent cells of the exodermis (in chickpea) or in the outermost cortex layer (in *M. truncatula* and *V. sativa*). Scale bar, 200 nm. SL: suberin lamellae; S: suberin; CW: cell wall; CP: cytoplasm. **d,** Quantification summary of PI diffusion in the roots of chickpea, *M. truncatula* and *V. sativa* treated with mock (black) or 2 µM ABA (red) for 3 days. For each species, the left images show representative confocal images of cross-section of roots, with the signal of PI diffusion across epidermal and cortex cells (scale = 25 µm). On the right, line plots show the relative pixel intensity of the cell wall PI dye in different layers of the root cortex (C1 to C5) relative to the intensity of the signal detected in the epidermis (EP). Asterisks indicate significance based on Wilcoxon rank-sum test with statistical significance of $P < 0.05$ ($n \geq 6$).

Figure 3. ABA induces temporally separated general ABA response and suberin biosynthesis programs in chickpea roots.

a, Simplified schematic diagram of suberin biosynthesis, transport and polymerization adapted from Cantó-Pastor *et al.* 2024. Black boxes indicate enzymes or transport proteins involved in each step of the pathway. FAs: fatty-acids; VLFA: very-long fatty-acids; KCS: 3-ketoacyl-CoA synthase; FAR: Fatty acyl-CoA reductase; CYP86A/B: cytochrome P450, family 86, subfamily A or B; LACS: laccases; GPAT: glycerol-3-phosphate acyltransferase; ASFT: Aliphatic suberin feruloyl-transferase; ABCG: ABC transporter G; LTP: lipid transfer protein; GELP: GDSL esterase/lipases. **b,** Schematic representations of time points (15, 30 and 45 min and 1, 2, 4, 6, 8 and 24 h) used to profile the transcriptome changes of roots (lower half of the root) from 3-day old chickpea treated with mock (grey) and 2μM ABA (red). **c**, Number of differentially expressed genes (DEGs) at each time point for ABA-treated roots compared with mock. DEGs were determined as genes with an Benjamini-Hochberg adjusted P value < 0.05 and log2FC > 1 (upregulated, pink) or log2FC < -1 (downregulated, blue). **d**, K-means clustering of DEGs (k = 8). The heatmap shows logFC values of each gene at each timepoint. For further analysis, we focused on the first four clusters that had the highest upregulation in response to ABA (Cluster I, II, III and IV). **e,** Expression patterns of representative genes from Cluster I (*Ca_04411: CaPKINASE*), II (*Ca_16115*: *CaGPAT5*), III (*Ca_14818*: *CaLAC2*) and IV (*Ca_06369: CaGELP*). **f**, Number of chickpea genes related to the canonical ABA response identified in Clusters I-IV. *LEA*: *LATE EMBRYOGENESIS ABUNDANT*; *PP2C*: *PROTEIN PHOSPHATASE 2C*; *RDB29B*: *RESPONSIVE TO DESICCATION 29B*. **g**, Number of chickpea genes related to suberin biosynthesis, transport and polymerization (listed in **a**) in Clusters I-IV.

Figure 4. Mechanisms of the temporal distinction between ABA response and suberin biosynthesis program in chickpea roots.

a, GBOX (CACGTG) and **b,** MYB (ACCTA) motif enrichment in the Cluster I-IV promoters (500 base pairs (bps) upstream the start codon (ATG) of each gene). Bar graphs show the percentage of promoters of DEGs (colored) and 1000 sets of promoters of randomly selected genes with equivalent number to the compared DEG list (grey) containing the indicated DNA motifs. A Bonferroni-adjusted P-value threshold of 0.01 was used to indicate the statistical significance (*) of enrichment, while ns indicates no significance. **c,d,** Schematic representation of position weight matrices (PWMs) identified through DAP-Seq of G-BOX BINDING FACTOR3 (GBF3) (navy blue) and MYB93 (red) TFs[45] detected by FIMO (p value < 0.001) in the promoters of ABA responsive genes in Cluster I (**c**) and in the promoters of suberin biosynthesis genes in Cluster II, III and IV (**d**). **e**, The temporal onset of *MYB* expression in response to ABA in chickpea roots. Red filled squares indicate significantly upregulated *MYBs* at each timepoint. **f**, Overview of the strategy used to evaluate the effect of ABA for the promoter activation of a *MYBs* that showed a rapid (*Ca_00232*) and delayed (*Ca_11228*) response to ABA in the time course RNA-seq experiment. The minimal *35S* promoter (*p35Sm*) and the promoter of *Ca_11449*, a gene that encodes for an ABA-responsive kinase (*pCaPKINASE*) were used as negative and positive controls, respectively. Gene constructs were transfected into Arabidopsis leaf protoplasts and incubated in mock or ABA (10 μM) treatments for 3 hours. **g**, Average ratios of Firefly to Renilla luciferase activity depicting the promoter activity in Arabidopsis leaf protoplasts incubated mock (black) or 10 μM ABA (red), with their respective standard deviation. Asterisks indicate significance based on Student's t-test with a P-value threshold of 0.05 (n = 3).

Figure 5. Single cell atlas of the chickpea root in response to ABA (2 Columns)

a, Overview of the scRNA-seq experiment in chickpea roots. 3-day-old chickpea seedlings were transferred to ½ MS medium plates containing 2μM ABA. After 24 hours, protoplasts were

released from roots (3 cm above the root tip) and loaded into the 10X Genomics Chromium chip for making the single-cell transcriptome libraries. **b**, Twenty-two clusters of the chickpea root cells in response to ABA. Here shown as an integrated UMAP with their respective annotated cell identities. **c**, Expression of the top 2 marker genes for each cluster. Dot size indicates the percentage of cells in the cluster that expresses the specific gene (% expressed). Dot colors represent the average scaled expression of genes in the clusters (Avg. expression). The top 2 markers were identified by looking at the genes with the lowest adjusted P-values and the greatest percentage differences with other clusters. In the bottom of the dotplot, a green filled square indicates if the marker gene has an orthologue annotated as a marker gene in equivalent cell type in the Arabidopsis root scPlantdb[48]. We manually curated the datasets in the scPlantdb by only keeping datasets in which *AtMYB36* was annotated as a marker for the endodermal cell cluster. **d**, Root cross section of chickpea roots grown in mock conditions stained with basic-fuchsin (BF) and calcofluor white. BF (blue) staining depicts the lignification of the Casparian strip in the root endodermis (green arrow). Calcofluor white (red) stains general cell-walls. **e**, Cross sections of chickpea roots grown with 2μM ABA stained with FY and counter-stained with aniline blue, showing that the suberin accumulation only occurs in the root exodermis (yellow arrow). Scale: 100 μm. **f**, Dotplot showing the spatial expression of Casparian strip related genes (left), suberin biosynthesis related genes (middle) and *MYBs* identified as upregulated in the time course bulk RNA-seq experiment.

Figure 6. Pseudotime estimation recapitulates the temporal dynamics of *CaMYB74* leading the differentiation of exodermis in chickpea roots

a, Cell lineage detection using the Slingshot package[52] revealed two lineages in the outer ground tissue (outer cortex and exodermis). The Meristem_1 cluster were included to help anchor the cell lineage detection and pseudotime estimations. Lineage 1 consists of clusters Meristem_1, Outercortex_1 and Exodermis_1, while Lineage 2 consists of Meristem_1, Outercortex_1 and Outercortex_2. **b**, Pseudotime trajectory through cell populations of Lineage 1. **c**, Scaled expression profiles of suberin biosynthesis, transport and polymerization genes along the Lineage 1 pseudotime trajectory. **d**, Scaled expression profiles of *MYBs* identified as upregulated by ABA in the time course bulk RNA-seq experiment. **e**, Our working model for the differentiation of chickpea exodermis has *CaMYB74* induced by ABA in multiple layers, whereas the putative downstream *MYBs* and suberin genes are expressed specifically in exodermis.

Supplementary figure legends

Supplementary Figure S1. Quantification summary of Basic Fuchsin (BF) dye intensity across multiple cell layers of legume roots in response to ABA. For each species, the top images show representative confocal images of cross-section of roots treated with mock or ABA (2 μM) for 3 days, with the signal of BF overlaid on top of bright field images (scale = 25 μm). The bottom heatmap shows the average pixel intensity of the BF signal in different layers of the root cross section. Asterisks indicate significance based on Wilcoxon rank-sum test with a Benjamini-Hochberg adjusted P-value threshold of 0.05 was used to indicate the statistical significance ($n \geq 8$).

Supplementary Figure S2. Suberin deposition in distinct developmental zones (25, 50 and 75% region of the root) in the exodermis/outer cortex or endodermis of chickpea (*C. arietinum*), pea (*L. oleraceus*), *V. sativa* and *M. truncatula* roots treated with mock or 2 μM ABA for 3 days. Pie charts depict the percentage of cross sections showing a non-suberized, an early-suberized (suberin in less than 50% of the cells in that layer), a late-suberized (suberin in more than 50% of cells in that layer), or diffuse (weak, non-specific) suberization pattern in the cortex.

Supplementary Figure S3. Bar charts showing the abundance (µg/mg of fresh-weight (FW)) of individual suberin monomers in roots treated with mock (grey) or 2 µM ABA (red) for 24 hours. Asterisks indicate significance based on Student's t-test with a P-value threshold of 0.05 (n = 4).

Supplementary Figure S4. TEM images of cross-sections at the 50% root region of Chickpea, *M. truncatula* and *V. sativa* treated with mock or 2 µM ABA for 3 days. The cell wall depicted in the images refer to the cell-wall between two adjacent endodermal cells. Scale bar, 200 nm. SL: suberin lamellae; CW: cell wall; CP: cytoplasm.

Supplementary Figure S5. Heatmap displaying the logFC values of genes associated with the putative general ABA response (**a**) and suberin biosynthesis and polymerization (**b**) across various time points of the ABA response in chickpea roots when compared to mock treatment.

Supplementary Figure S6. Representative confocal images of cross-sections of roots used for the time course RNA-seq experiment: treated with mock or 2 µM ABA at two distinct time points (6 and 24 hours), with the signal of FY overlaid on top of bright field images (scale = 100 µm).

Supplementary Figure S7. Enrichment of ATHB7 (ATNATTG), bHLH122 (CNACTTG), NF-YA (CCAAT), ANAC058 (CNTNNNNNNNANG), WRKY40 (TTGACT) and HAT5 (AATAATT) DNA binding motifs in the promoters of DEGs in clusters I, II, III and IV. Bar graphs show the percentage of promoters of DEGs (colored) and 1000 sets of promoters of randomly selected genes with equivalent number in the compared DEG list (grey) containing the indicated DNA motifs. A Bonferroni-adjusted P-value threshold of 0.01 was used to indicate the statistical significance (*) of enrichment, while ns indicates no significance.

Supplementary Figure S8. Representative phylogenetic tree showing the closest Arabidopsis homologs to chickpea MYBs TFs identified as upregulated by ABA in the time course bulk RNA-seq experiment. Full length amino acid sequences of chickpea upregulated MYBs and all annotated Arabidopsis MYB TFs were aligned using MAFFT. The phylogenetic tree was determined using the maximum likelihood method with 1000 bootstraps using iQ-TREE. Distant nodes where chickpea MYB TFs were not detected were removed to improve the visualization of the cladogram. Upregulated MYBs are indicated in red, and the TAIR10 symbol respective to close orthologues are indicated.

Supplementary Figure S9. Reproducibility of single-cell chickpea root atlas in response to ABA as observed by UMAP (**a**), markers identified (**b**), and profile of expression of Casparian strip related genes (**c**) and suberin biosynthesis genes (**d**). Two independent experiments (Exp1 (blue) and Exp2 (salmon)) that generated individual single-cell libraries from protoplasts isolated from chickpea roots grown in the presence of 2 µM ABA, Exp1 for 24h and Exp2 for 48h. Dot size indicates the percentage of cells in the cluster that expresses the specific gene (% expressed). Dot colors represent the average scaled expression of genes in the clusters (Avg. expression).

Supplementary Figure S10. Bar plots showing the percentage of chickpea genes in each annotated single-cell cluster that has at least one orthologue identified as a marker in the Arabidopsis root scPlantdb cluster from cell representing dividing cells (a), xylem (b), phloem (c), pericycle (d), ground tissue (e), epidermis (f) and root cap (g). We manually curated the datasets in the scPlantdb by only keeping datasets in which *AtMYB36* was annotated as a marker for the endodermal cell cluster.

Supplementary Figure S11. a, Top: UMAP profile showing the scaled expression of orthologue genes to characterized markers in Arabidopsis by Shahan et al. 2022. Bottom: UMAP profile showing the scaled expression of marker genes in Arabidopsis phloem, endodermis and cortex[49]. **b**, Dotplot showing the spatial expression of chickpea orthologues of empirically determined root cell markers in Arabidopsis determined by Shahan et al. 2022.

Supplementary Figure S12. Dotplot showing the spatial expression of genes found in Cluster I, II, III and IV, based on the K-means clustering analysis of the time course bulk-RNAseq experiment in chickpea roots in response to ABA.

Supplementary Figure 13 UMAP profile showing the scaled expression of select putative ABA responsive genes in the single-cell atlas of chickpea roots grown on 2 μM ABA for 24h.

References

1. Barberon, M. *et al.* Adaptation of root function by nutrient-induced plasticity of endodermal differentiation. *Cell* **164**, 447–459 (2016).
2. Shukla, V. *et al.* Suberin plasticity to developmental and exogenous cues is regulated by a set of MYB transcription factors. *Proc. Natl. Acad. Sci. U. S. A.* **118**, e2101730118 (2021).
3. Cantó-Pastor, A. *et al.* A suberized exodermis is required for tomato drought tolerance. *Nat. Plants* **10**, 118–130 (2024).
4. Chen, X. *et al.* Four MYB transcription factors regulate suberization and non-localized lignification at the root endodermis in rice. *Plant Cell* (2024) doi:10.1093/plcell/koae278.
5. Shiono, K. *et al.* Abscisic acid is required for exodermal suberization to form a barrier to radial oxygen loss in the adventitious roots of rice (Oryza sativa). *New Phytol.* **233**, 655–669 (2022).
6. Su, Y. *et al.* The evolutionary innovation of root suberin lamellae contributed to the rise of seed plants. *Nat. Plants* **9**, 1968–1977 (2023).
7. Manzano, C. *et al.* Regulation and function of a polarly localized lignin barrier in the exodermis. *Nat. Plants* (2024) doi:10.1038/s41477-024-01864-z.
8. Alassimone, J., Naseer, S. & Geldner, N. A developmental framework for endodermal differentiation and polarity. *Proc. Natl. Acad. Sci. U. S. A.* **107**, 5214–5219 (2010).
9. Roppolo, D. *et al.* A novel protein family mediates Casparian strip formation in the endodermis. *Nature* **473**, 380–383 (2011).
10. Hosmani, P. S. *et al.* Dirigent domain-containing protein is part of the machinery required for formation of the lignin-based Casparian strip in the root. *Proc. Natl. Acad. Sci. U. S. A.* **110**, 14498–14503 (2013).
11. Lee, Y., Rubio, M. C., Alassimone, J. & Geldner, N. A mechanism for localized lignin deposition in the endodermis. *Cell* **153**, 402–412 (2013).
12. Doblas, V. G. *et al.* Root diffusion barrier control by a vasculature-derived peptide binding to the SGN3 receptor. *Science* **355**, 280–284 (2017).
13. Nakayama, T. *et al.* A peptide hormone required for Casparian strip diffusion barrier formation in Arabidopsis roots. *Science* **355**, 284–286 (2017).
14. Naseer, S. *et al.* Casparian strip diffusion barrier in Arabidopsis is made of a lignin polymer without suberin. *Proc. Natl. Acad. Sci. U. S. A.* **109**, 10101–10106 (2012).
15. Barberon, M. The endodermis as a checkpoint for nutrients. *New Phytol.* **213**, 1604–1610 (2017).
16. Geldner, N. The endodermis. *Annu. Rev. Plant Biol.* **64**, 531–558 (2013).
17. Andersen, T. G. & Drapek, C. The endodermis 1. in *Plant Roots* 90–103 (CRC Press, Boca Raton, 2024).
18. Liu, T. & Kreszies, T. The exodermis: A forgotten but promising apoplastic barrier. *J. Plant Physiol.* **290**, 154118 (2023).
19. Perumalla, C. J., Peterson, C. A. & Enstone, D. E. A survey of angiosperm species to detect hypodermal Casparian bands. I. Roots with a uniseriate hypodermis and epidermis. *Bot. J. Linn. Soc.* **103**, 93–112 (1990).
20. Peterson, C. A. & Perumalla, C. J. A survey of angiosperm species to detect hypodermal Casparian bands. II. Roots with a multiseriate hypodermis or epidermis. *Bot. J. Linn. Soc.* **103**, 113–125 (1990).

21. Perumalla, C. J., Chmielewski, J. G. & Peterson, C. A. A survey of angiosperm species to detect hypodermal Casparian bands. III. Rhizomes. *Bot. J. Linn. Soc.* **103**, 127–132 (1990).
22. Baumgart, L. A. *et al.* An atlas of conserved transcription factor binding sites reveals the cell type-resolved gene regulatory landscape of flowering plants. *bioRxiv* (2024) doi:10.1101/2024.10.08.617089.
23. Lashbrooke, J. *et al.* MYB107 and MYB9 homologs regulate suberin deposition in angiosperms. *Plant Cell* **28**, 2097–2116 (2016).
24. Dubos, C. *et al.* MYB transcription factors in Arabidopsis. *Trends Plant Sci.* **15**, 573–581 (2010).
25. Du, H. *et al.* The evolutionary history of R2R3-MYB proteins across 50 eukaryotes: New insights into subfamily classification and expansion. *Sci. Rep.* **5**, 11037 (2015).
26. Xu, H. *et al.* Transcriptional networks regulating suberin and lignin in endodermis link development and ABA response. *Plant Physiol.* **190**, 1165–1181 (2022).
27. Cohen, H., Fedyuk, V., Wang, C., Wu, S. & Aharoni, A. SUBERMAN regulates developmental suberization of the Arabidopsis root endodermis. *Plant J.* **102**, 431–447 (2020).
28. Jo, L. *et al.* Transcription factors SlMYB41, SlMYB92 and SlWRKY71 regulate gene expression in the tomato exodermis. *bioRxiv* (2024) doi:10.1101/2024.08.29.610307.
29. Artur, M. A. S. & Kajala, K. Convergent evolution of gene regulatory networks underlying plant adaptations to dry environments. *Plant Cell Environ.* **44**, 3211–3222 (2021).
30. Enstone, D. E., Peterson, C. A. & Ma, F. Root endodermis and exodermis: Structure, function, and responses to the environment. *J. Plant Growth Regul.* **21**, 335–351 (2002).
31. Taleisnik, E. Water retention capacity in root segments differing in the degree of exodermis development. *Ann. Bot.* **83**, 19–27 (1999).
32. Bani, M., Pérez-De-Luque, A., Rubiales, D. & Rispail, N. Physical and Chemical Barriers in Root Tissues Contribute to Quantitative Resistance to Fusarium oxysporum f. sp. pisi in Pea. *Front. Plant Sci.* **9**, 199 (2018).
33. Sharma, N. K. *et al.* MicroRNA397 regulates tolerance to drought and fungal infection by regulating lignin deposition in chickpea root. *Plant Cell Environ.* **46**, 3501–3517 (2023).
34. Schreiber, L., Hartmann, K., Skrabs, M. & Zeier, J. Apoplastic barriers in roots: chemical composition of endodermal and hypodermal cell walls. *J. Exp. Bot.* **50**, 1267–1280 (1999).
35. Brundrett, M. C., Kendrick, B. & Peterson, C. A. Efficient lipid staining in plant material with sudan red 7B or fluorol [correction of fluoral] yellow 088 in polyethylene glycol-glycerol. *Biotech. Histochem.* **66**, 111–116 (1991).
36. Lux, A., Morita, S., Abe, J. & Ito, K. An improved method for clearing and staining free-hand sections and whole-mount samples. *Ann. Bot.* **96**, 989–996 (2005).
37. Heslop-Harrison, Y., Heslop-Harrison, J. S. & Heslop-Harrison, J. Germination of Corylus Avellana l. (Hazel) pollen: Hydration and the function of the oncus. *Acta Bot. Neerl.* **35**, 265–284 (1986).
38. Dharmawardhana, D. P., Ellis, B. E. & Carlson, J. E. Characterization of vascular lignification in Arabidopsis thaliana. *Can. J. Bot.* **70**, 2238–2244 (1992).
39. Falk, H. & El-Hadidi, M. N. Der Feinbau der Suberinschichten verkorkter Zellwände. *Z. Naturforsch. B J. Chem. Sci.* **16**, 134–137 (1961).
40. Serra, O. & Geldner, N. The making of suberin. *New Phytol.* **235**, 848–866 (2022).
41. Guiltinan, M. J., Marcotte, W. R., Jr & Quatrano, R. S. A plant leucine zipper protein that recognizes an abscisic acid response element. *Science* **250**, 267–271 (1990).
42. Choi, H., Hong, J., Ha, J., Kang, J. & Kim, S. Y. ABFs, a family of ABA-responsive element binding factors. *J. Biol. Chem.* **275**, 1723–1730 (2000).
43. Ng, L. M., Melcher, K., Teh, B. T. & Xu, H. E. Abscisic acid perception and signaling: structural mechanisms and applications. *Acta Pharmacol. Sin.* **35**, 567–584 (2014).
44. Zenker, S. *et al.* Many transcription factor families have evolutionarily conserved binding motifs in plants. *bioRxiv* (2024) doi:10.1101/2024.10.31.621407.

45. O'Malley, R. C. *et al*. Cistrome and epicistrome features shape the regulatory DNA landscape. *Cell* **166**, 1598 (2016).
46. Ortiz-García, P. *et al*. The indole-3-acetamide-induced Arabidopsis transcription factor MYB74 decreases plant growth and contributes to the control of osmotic stress responses. *Front. Plant Sci.* **13**, 928386 (2022).
47. Kosma, D. K. *et al*. AtMYB41 activates ectopic suberin synthesis and assembly in multiple plant species and cell types. *Plant J.* **80**, 216–229 (2014).
48. He, Z. *et al*. scPlantDB: a comprehensive database for exploring cell types and markers of plant cell atlases. *Nucleic Acids Res.* **52**, D1629–D1638 (2024).
49. Shahan, R. *et al*. A single-cell Arabidopsis root atlas reveals developmental trajectories in wild-type and cell identity mutants. *Dev. Cell* **57**, 543-560.e9 (2022).
50. Liberman, L. M., Sparks, E. E., Moreno-Risueno, M. A., Petricka, J. J. & Benfey, P. N. MYB36 regulates the transition from proliferation to differentiation in the Arabidopsis root. *Proc. Natl. Acad. Sci. U. S. A.* **112**, 12099–12104 (2015).
51. Kamiya, T. *et al*. The MYB36 transcription factor orchestrates Casparian strip formation. *Proc. Natl. Acad. Sci. U. S. A.* **112**, 10533–10538 (2015).
52. Street, K. *et al*. Slingshot: cell lineage and pseudotime inference for single-cell transcriptomics. *BMC Genomics* **19**, (2018).
53. Kreplak, J. *et al*. A reference genome for pea provides insight into legume genome evolution. *Nat. Genet.* **51**, 1411–1422 (2019).
54. Silva-Navas, J. *et al*. D-Root: a system for cultivating plants with the roots in darkness or under different light conditions. *Plant J.* **84**, 244–255 (2015).
55. Krueger, F. A wrapper tool around Cutadapt and FastQC to consistently apply quality and adapter trimming to FastQ files 516. **517**, (2015).
56. Bray, N. L., Pimentel, H., Melsted, P. & Pachter, L. Near-optimal probabilistic RNA-seq quantification. *Nat. Biotechnol.* **34**, 525–527 (2016).
57. Ritchie, M. E. *et al*. limma powers differential expression analyses for RNA-sequencing and microarray studies. *Nucleic Acids Res.* **43**, e47 (2015).
58. Robinson, M. D., McCarthy, D. J. & Smyth, G. K. edgeR: a Bioconductor package for differential expression analysis of digital gene expression data. *Bioinformatics* **26**, 139–140 (2010).
59. Jo, L. *et al*. Combinatorial interactions of the LEC1 transcription factor specify diverse developmental programs during soybean seed development. *Proc. Natl. Acad. Sci. U. S. A.* **117**, 1223–1232 (2020).
60. Quinlan, A. R. & Hall, I. M. BEDTools: a flexible suite of utilities for comparing genomic features. *Bioinformatics* **26**, 841–842 (2010).
61. Hao, Y. *et al*. Dictionary learning for integrative, multimodal and scalable single-cell analysis. *Nat. Biotechnol.* **42**, 293–304 (2024).
62. Young, M. D. & Behjati, S. SoupX removes ambient RNA contamination from droplet-based single-cell RNA sequencing data. *Gigascience* **9**, (2020).
63. Germain, P.-L. *ScDblFinder*. (Bioconductor, 2019). doi:10.18129/B9.BIOC.SCDBLFINDER.
64. Cannon, S. B. *et al*. Polyploidy did not predate the evolution of nodulation in all legumes. *PLoS One* **5**, e11630 (2010).
65. Ellis, T. H. N. *et al*. The taxonomic status of genera within the Fabeae (Vicieae), with a special focus on Pisum. *Diversity (Basel)* **16**, 365 (2024).

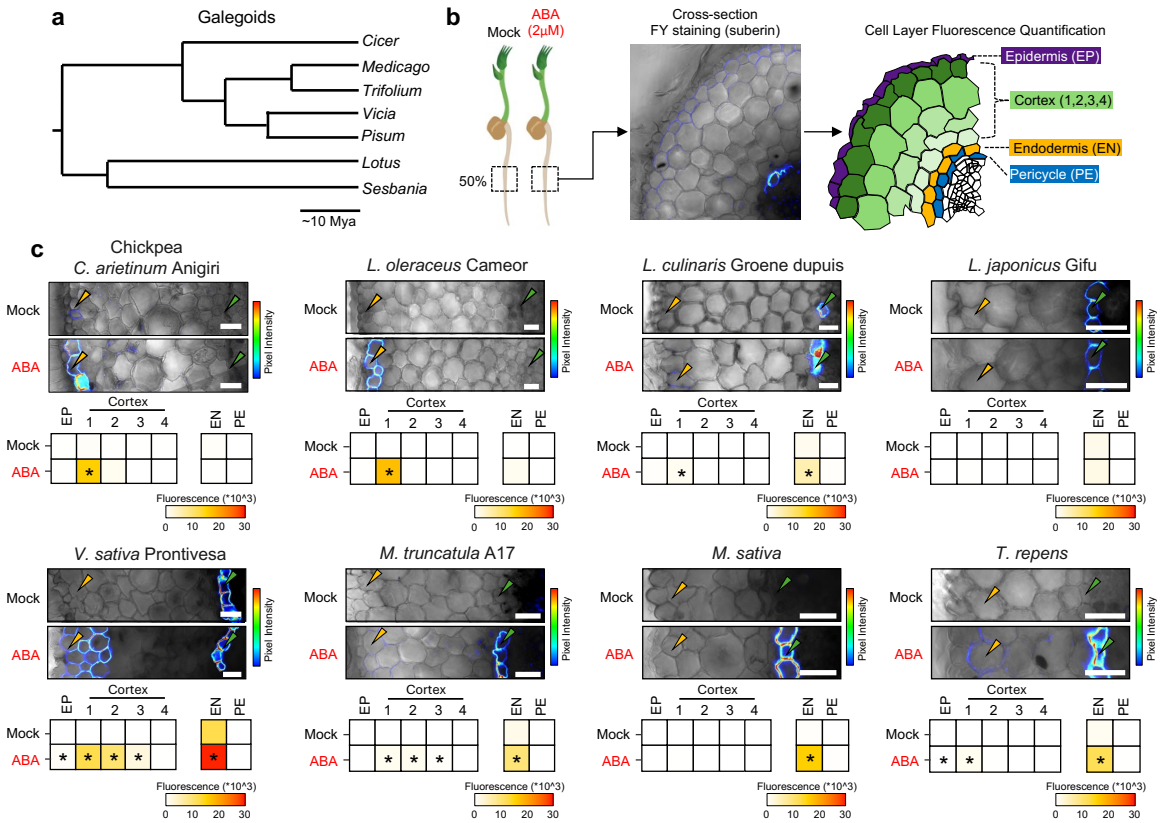

Figure 1. Galegoid legumes deposit suberin to the cell walls of different root cell types in response to ABA. a, Representative phylogenetic tree of the galegoid legume clade. The tree was adapted from[63]. Species marked with an arrow correspond to species used in this study. *Lens culinaris* is nested in the genus *Vicia*[64]. **b,** Graphical representation of the survey for observing cell-type suberization in legume roots treated with mock or ABA (2 μM) for 3 days. The middle point of the root (50%) was cross-sectioned, stained with FY and counter-stained with aniline blue. Finally, the fluorescence levels of cell walls of individual cell layers of the root epidermis (EP), the four outermost cell layers of the cortex (C1 to C4), the endodermis (EN) and the pericycle (PE) were quantified. **c,** Quantification summary of FY intensity across multiple cell layers of legume roots in response to ABA. For each species, the top images show representative confocal images of cross-section of roots treated with mock or ABA, with the FY signal overlaid on top of bright field images (scale = 25 μm). The yellow and green arrow depicts the position of the outermost layer of the cortex and endodermis, respectively. On the bottom, the heatmaps show the average pixel intensity of the FY signal in different layers of the root cross section. Asterisks indicate significance based on Wilcoxon rank-sum test with a Benjamini-Hochberg adjusted P-value. Threshold of 0.05 was used to indicate the statistical significance ($n \geq 8$).

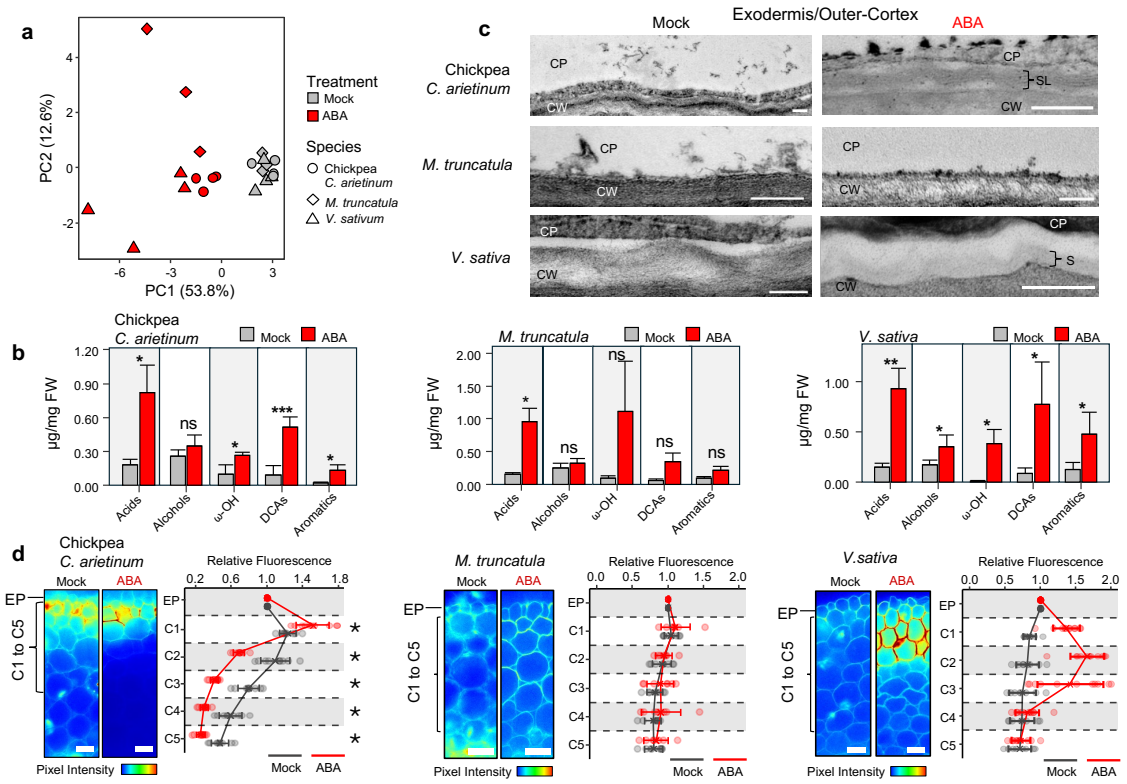

Figure 2. Biochemical, structural and functional evaluation of ABA-induced cell wall modifications show that chickpea forms an exodermis with a suberin lamella and an apoplastic diffusion barrier. a, Principal Component Analysis (PCA) of suberin monomer abundances in roots of chickpea, *M. truncatula* and *V. sativa* treated with mock or 2 µM ABA for 24 hours. **b,** Abundance of major classes of suberin monomers in roots treated with mock (grey) or 2 µM ABA (red) for 24 hours. Asterisks indicate significance based on Student's t-test with a P-value threshold of 0.05 (n = 4). **c,** Transmission electron microscopy (TEM) cross-sections at the 50% region of Chickpea, *M. truncatula* and *V. sativa* roots treated with mock or 2 µM ABA for 3 days. The cell wall (CW) depicted in the images refers to the cell wall between two adjacent cells of the exodermis (in chickpea) or in the outermost cortex layer (in *M. truncatula* and *V. sativa*). Scale bar, 200 nm. SL: suberin lamellae; S: suberin; CW: cell wall; CP: cytoplasm. **d,** Quantification summary of PI diffusion in the roots of chickpea, *M. truncatula* and *V. sativa* treated with mock (black) or 2 µM ABA (red) for 3 days. For each species, the left images show representative confocal images of cross-section of roots, with the signal of PI diffusion across epidermal and cortex cells (scale = 25 µm). On the right, line plots show the relative pixel intensity of the cell wall PI dye in different layers of the root cortex (C1 to C5) relative to the intensity of the signal detected in the epidermis (EP). Asterisks indicate significance based on Wilcoxon rank-sum test with statistical significance of $P < 0.05$ ($n \geq 6$).

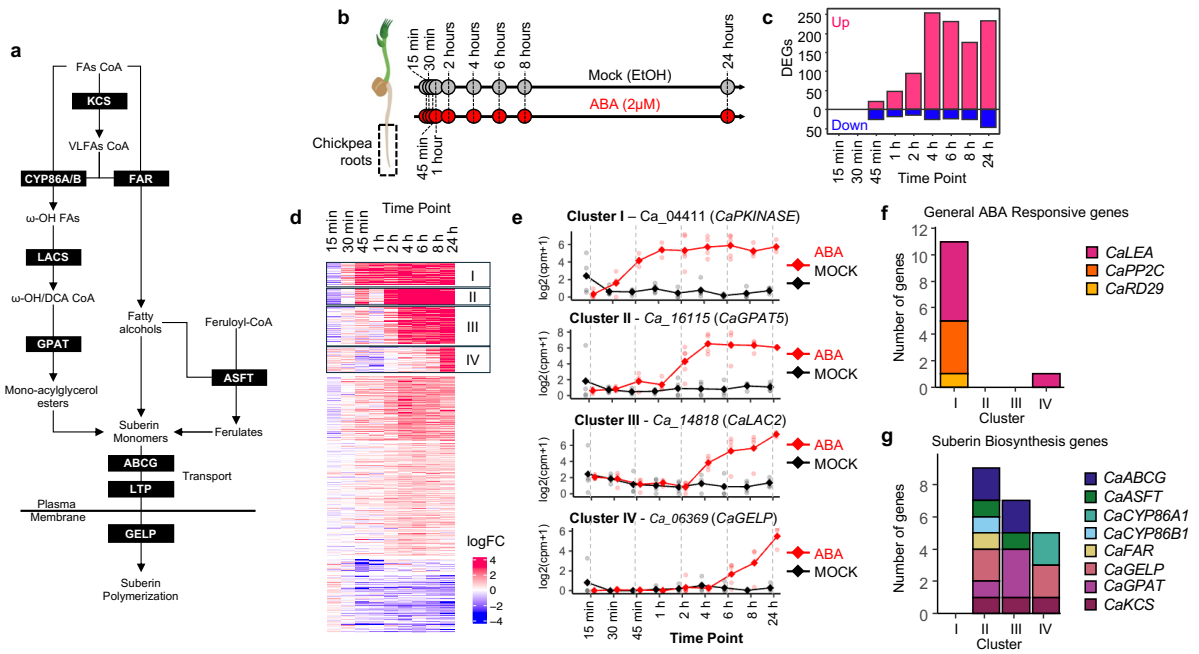

Figure 3. ABA induces temporally separated general ABA response and suberin biosynthesis programs in chickpea roots.

a, Simplified schematic diagram of suberin biosynthesis, transport and polymerization adapted from Canto-Pastor *et al.* 2024. Black boxes indicate enzymes or transport proteins involved in each step of the pathway. FAs: fatty-acids; VLFA: very-long fatty-acids; KCS: 3-ketoacyl-CoA synthase; FAR: Fatty acyl-CoA reductase; CYP86A/B: cytochrome P450, family 86, subfamily A or B; LACS: laccases; GPAT: glycerol-3-phosphate acyltransferase; ASFT: Aliphatic suberin feruloyl-transferase; ABCG: ABC transporter G; LTP: lipid transfer protein; GELP: GDSL esterase/lipases. **b,** Schematic representations of time points (15, 30 and 45 min and 1, 2, 4, 6, 8 and 24 h) used to profile the transcriptome changes of roots (lower half of the root) from 3-day old chickpea treated with mock (grey) and 2µM ABA (red). **c**, Number of differentially expressed genes (DEGs) at each time point for ABA-treated roots compared with mock. DEGs were determined as genes with an Benjamini-Hochberg adjusted P value < 0.05 and log2FC > 1 (upregulated, pink) or log2FC < -1 (downregulated, blue). **d**, K-means clustering of DEGs (k = 8). The heatmap shows logFC values of each gene at each timepoint. For further analysis, we focused on the first four clusters that had the highest upregulation in response to ABA (Cluster I, II, III and IV). **e,** Expression patterns of representative genes from Cluster I (*Ca_04411: CaPKINASE*), II (*Ca_16115*: *CaGPAT5*), III (*Ca_14818*: *CaLAC2*) and IV (*Ca_06369: CaGELP*). **f**, Number of chickpea genes related to the canonical ABA response identified in Clusters I-IV. *LEA*: *LATE EMBRYOGENESIS ABUNDANT*; *PP2C*: *PROTEIN PHOSPHATASE 2C*; *RDB29B*: *RESPONSIVE TO DESICCATION 29B*. **g**, Number of chickpea genes related to suberin biosynthesis, transport and polymerization (listed in **a**) in Clusters I-IV.

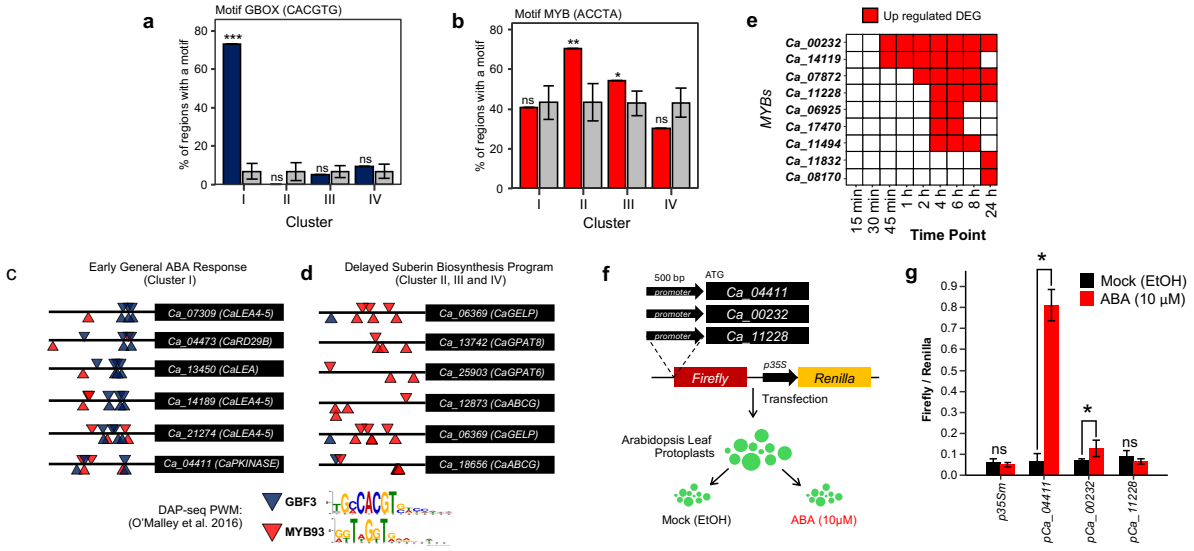

Figure 4. Mechanisms of the temporal distinction between ABA response and suberin biosynthesis program in chickpea roots.

a, GBOX (CACGTG) and **b,** MYB (ACCTA) motif enrichment in the Cluster I-IV promoters (500 base pairs (bps) upstream the start codon (ATG) of each gene). Bar graphs show the percentage of promoters of DEGs (colored) and 1000 sets of promoters of randomly selected genes with equivalent number to the compared DEG list (grey) containing the indicated DNA motifs. A Bonferroni-adjusted P-value threshold of 0.01 was used to indicate the statistical significance (*) of enrichment, while ns indicates no significance. **c,d,** Schematic representation of position weight matrices (PWMs) identified through DAP-Seq of G-BOX BINDING FACTOR3 (GBF3) (navy blue) and MYB93 (red) TFs[45] detected by FIMO (p value < 0.001) in the promoters of ABA responsive genes in Cluster I (**c**) and in the promoters of suberin biosynthesis genes in Cluster II, III and IV (**d**). **e**, The temporal onset of *MYB* expression in response to ABA in chickpea roots. Red filled squares indicate significantly upregulated *MYBs* at each timepoint. **f**, Overview of the strategy used to evaluate the effect of ABA for the promoter activation of a *MYBs* that showed a rapid (*Ca_00232*) and delayed (*Ca_11228*) response to ABA in the time course RNA-seq experiment. The minimal *35S* promoter (*p35Sm*) and the promoter of *Ca_11449*, a gene that encodes for an ABA-responsive kinase (*pCaPKINASE*) were used as negative and positive controls, respectively. Gene constructs were transfected into Arabidopsis leaf protoplasts and incubated in mock or ABA (10 μM) treatments for 3 hours. **g**, Average ratios of Firefly to Renilla luciferase activity depicting the promoter activity in Arabidopsis leaf protoplasts incubated mock (black) or 10 μM ABA (red), with their respective standard deviation. Asterisks indicate significance based on Student's t-test with a P-value threshold of 0.05 (n = 3).

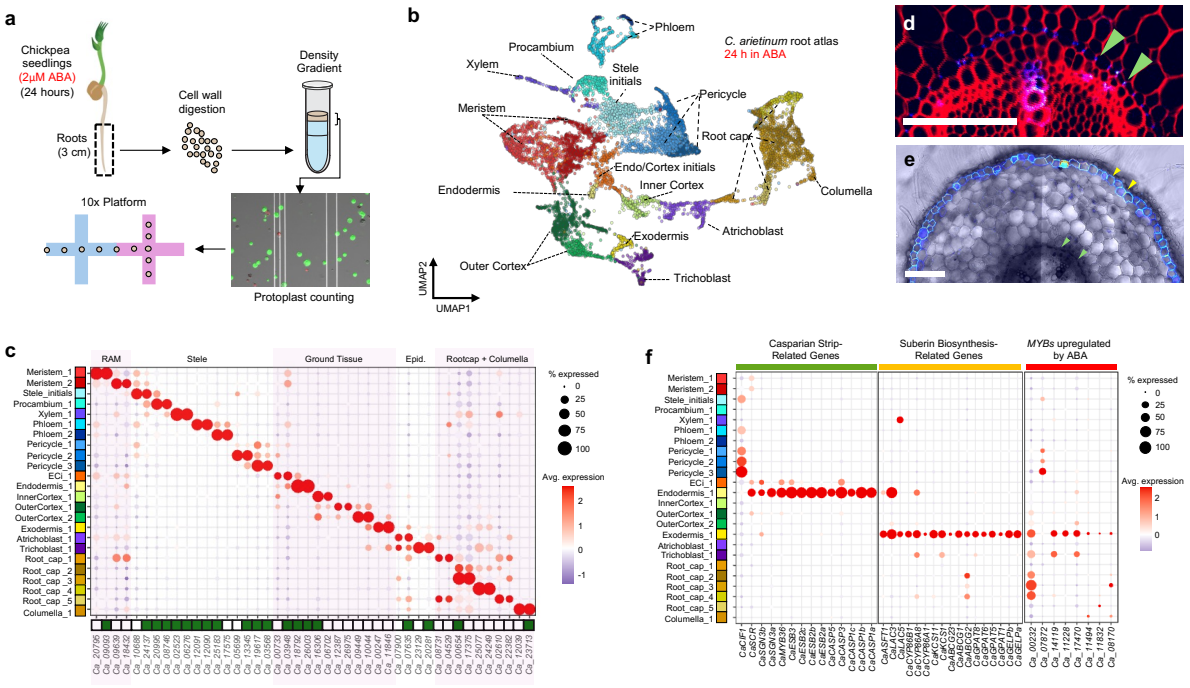

Figure 5. Single cell atlas of the chickpea root in response to ABA (2 Columns)

a, Overview of the scRNA-seq experiment in chickpea roots. 3-day-old chickpea seedlings were transferred to ½ MS medium plates containing 2μM ABA. After 24 hours, protoplasts were released from roots (3 cm above the root tip) and loaded into the 10X Genomics Chromium chip for making the single-cell transcriptome libraries. **b**, Twenty-two clusters of the chickpea root cells in response to ABA. Here shown as an integrated UMAP with their respective annotated cell identities. **c**, Expression of the top 2 marker genes for each cluster. Dot size indicates the percentage of cells in the cluster that expresses the specific gene (% expressed). Dot colors represent the average scaled expression of genes in the clusters (Avg. expression). The top 2 markers were identified by looking at the genes with the lowest adjusted P-values and the greatest percentage differences with other clusters. In the bottom of the dotplot, a green filled square indicates if the marker gene has an orthologue annotated as a marker gene in equivalent cell type in the Arabidopsis root scPlantdb[48]. We manually curated the datasets in the scPlantdb by only keeping datasets in which *AtMYB36* was annotated as a marker for the endodermal cell cluster. **d**, Root cross section of chickpea roots grown in mock conditions stained with basic-fuchsin (BF) and calcofluor white. BF (blue) staining depicts the lignification of the Casparian strip in the root endodermis (green arrow). Calcofluor white (red) stains general cell-walls. **e**, Cross sections of chickpea roots grown with 2μM ABA stained with FY and counter-stained with aniline blue, showing that the suberin accumulation only occurs in the root exodermis (yellow arrow). Scale: 100 μm. **f**, Dotplot showing the spatial expression of Casparian strip related genes (left), suberin biosynthesis related genes (middle) and *MYBs* identified as upregulated in the time course bulk RNA-seq experiment.

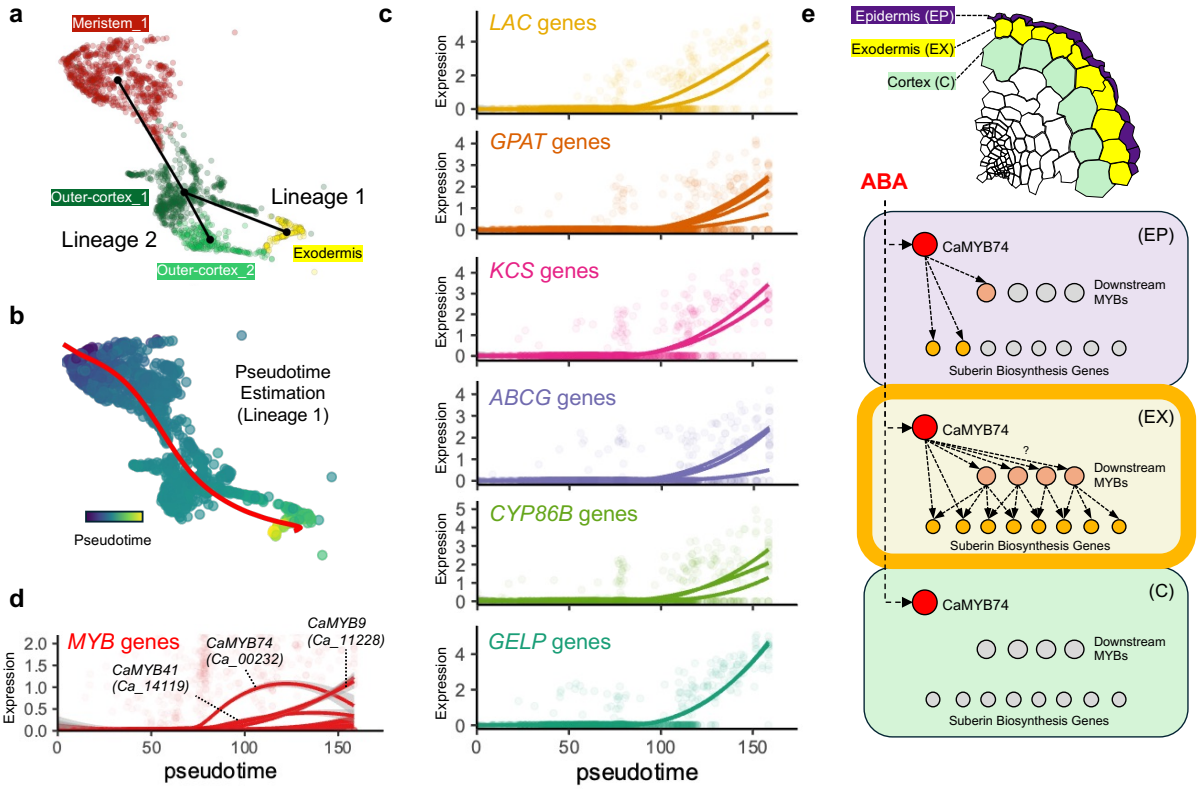

Figure 6. Pseudotime estimation recapitulates the temporal dynamics of *CaMYB74* leading the differentiation of exodermis in chickpea roots

a, Cell lineage detection using the Slingshot package[52] revealed two lineages in the outer ground tissue (outer cortex and exodermis). The Meristem_1 cluster were included to help anchor the cell lineage detection and pseudotime estimations. Lineage 1 consists of clusters Meristem_1, Outercortex_1 and Exodermis_1, while Lineage 2 consists of Meristem_1, Outercortex_1 and Outercortex_2. **b**, Pseudotime trajectory through cell populations of Lineage 1. **c**, Scaled expression profiles of suberin biosynthesis, transport and polymerization genes along the Lineage 1 pseudotime trajectory. **d**, Scaled expression profiles of *MYBs* identified as upregulated by ABA in the time course bulk RNA-seq experiment. **e**, Our working model for the differentiation of chickpea exodermis has *CaMYB74* induced by ABA in multiple layers, whereas the putative downstream *MYBs* and suberin genes are expressed specifically in exodermis.

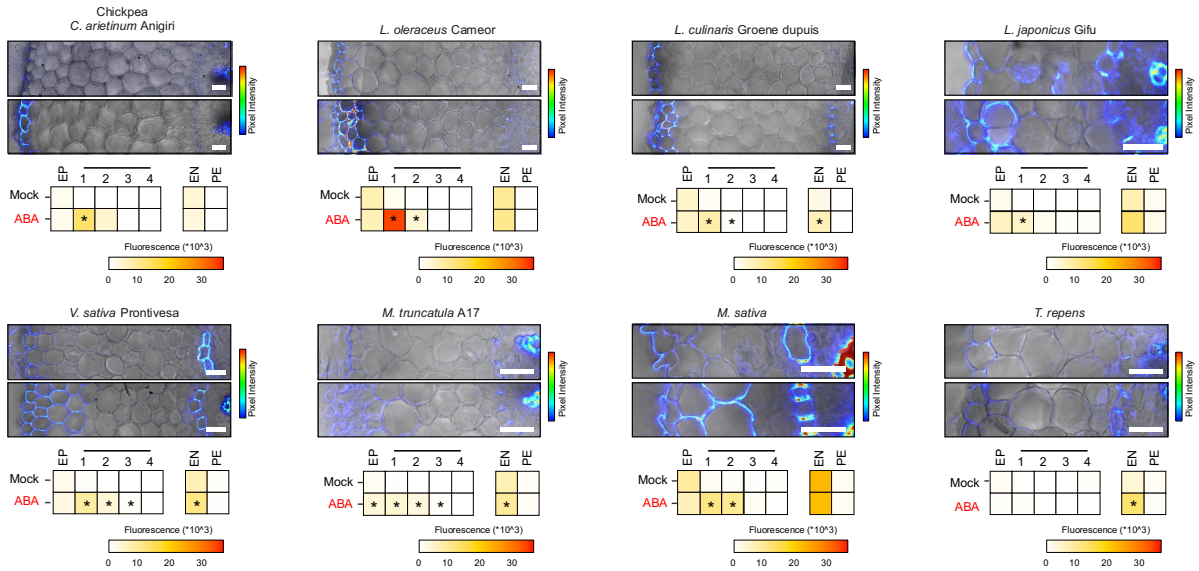

Supplementary Figure S1. Quantification summary of Basic Fuchsin (BF) dye intensity across multiple cell layers of legume roots in response to ABA. For each species, the top images show representative confocal images of cross-section of roots treated with mock or ABA (2 μM) for 3 days, with the signal of BF overlaid on top of bright field images (scale = 25 μm). The bottom heatmap shows the average pixel intensity of the BF signal in different layers of the root cross section. Asterisks indicate significance based on Wilcoxon rank-sum test with a Benjamini-Hochberg adjusted P-value threshold of 0.05 was used to indicate the statistical significance ($n \geq 8$).

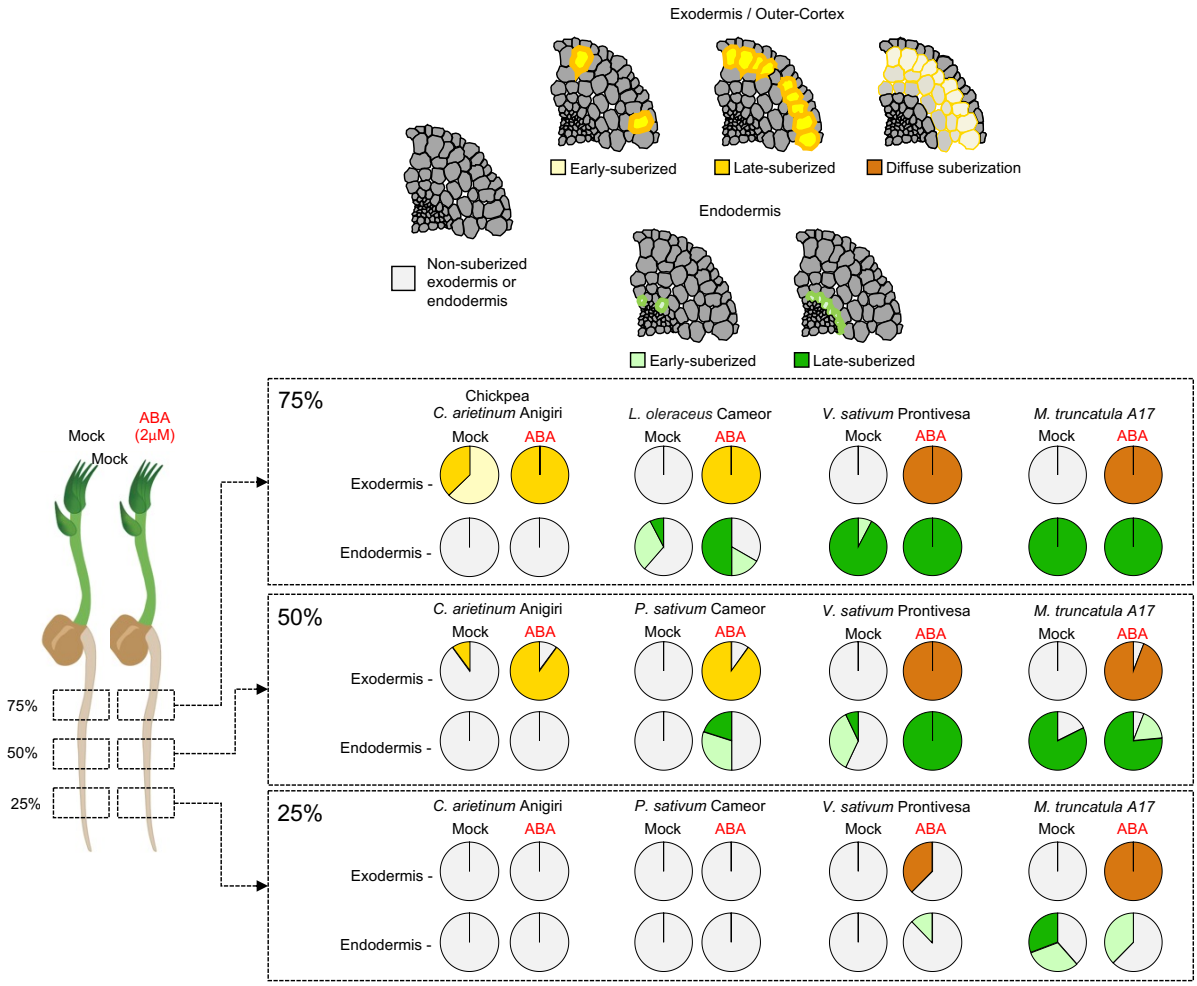

Supplementary Figure S2. Suberin deposition in distinct developmental zones (25, 50 and 75% region of the root) in the exodermis/outer cortex or endodermis of chickpea (*C. arietinum*), pea (*L. oleraceus*), *V. sativa* and *M. truncatula* roots treated with mock or 2 µM ABA for 3 days. Pie charts depict the percentage of cross sections showing a non-suberized, an early-suberized (suberin in less than 50% of the cells in that layer), a late-suberized (suberin in more than 50% of cells in that layer), or diffuse (weak, non-specific) suberization pattern in the cortex.

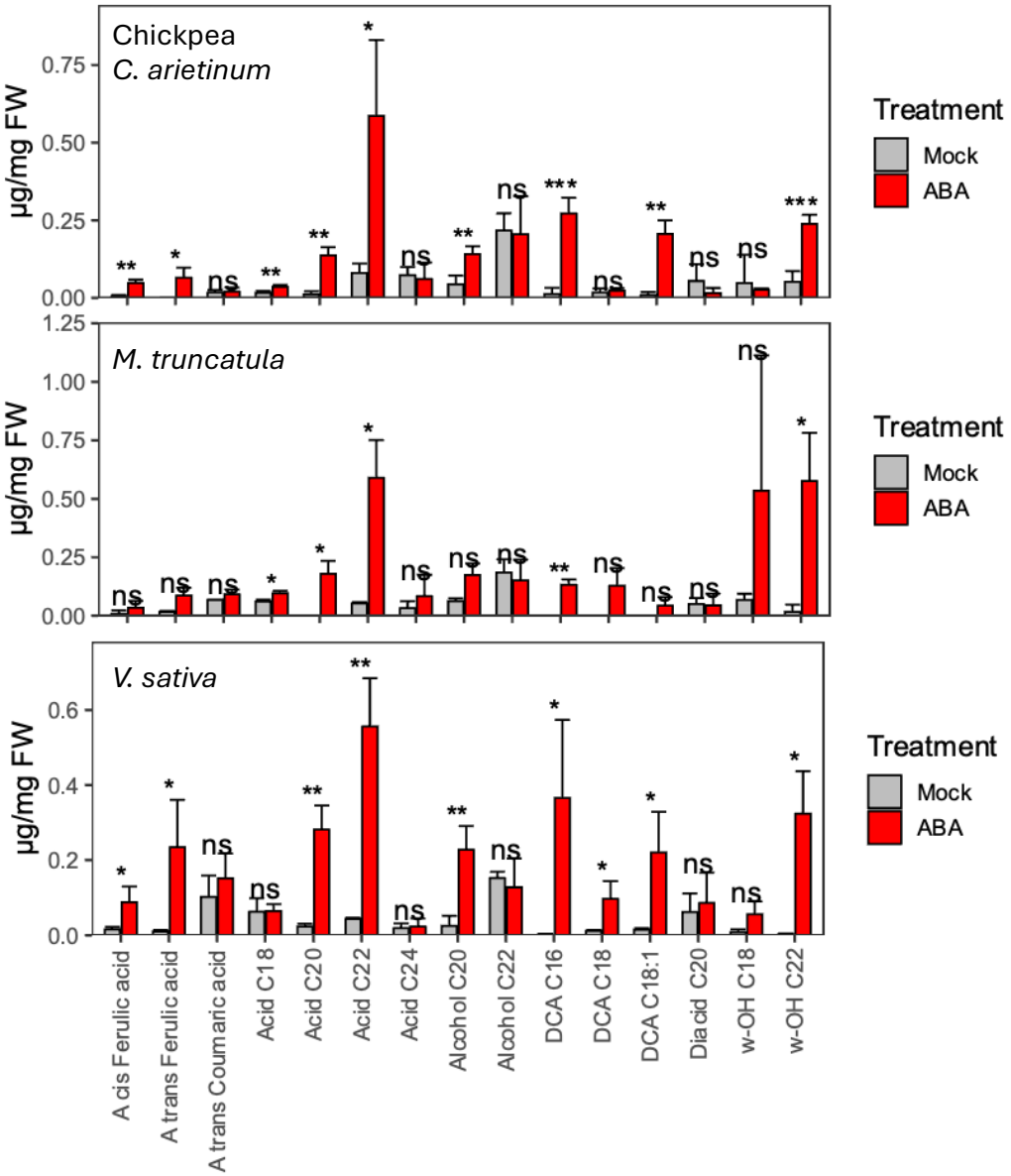

Supplementary Figure S3. Bar charts showing the abundance (µg/mg of fresh-weight (FW)) of individual suberin monomers in roots treated with mock (grey) or 2 µM ABA (red) for 24 hours. Asterisks indicate significance based on Student's t-test with a P-value threshold of 0.05 (n = 4).

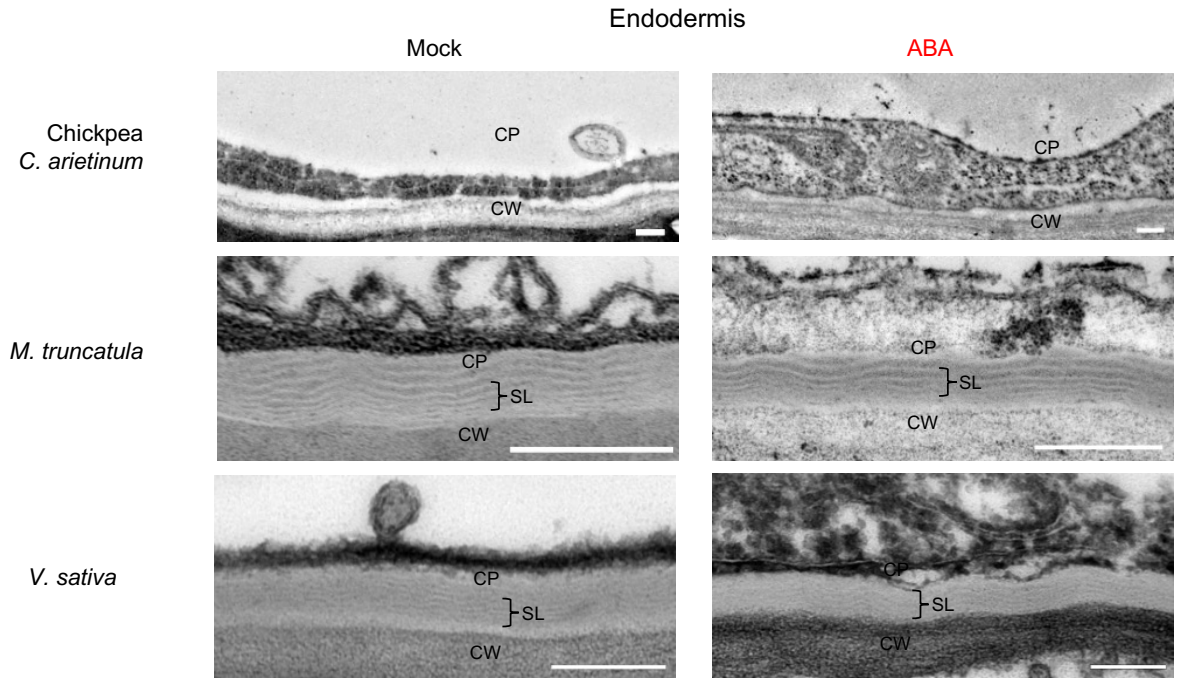

Supplementary Figure S4. TEM images of cross-sections at the 50% root region of Chickpea, *M. truncatula* and *V. sativa* treated with mock or 2 µM ABA for X days. The cell wall depicted in the images refer to the cell-wall between two adjacent endodermal cells. Scale bar, 200 nm. SL: suberin lamellae; CW: cell wall; CP: cytoplasm.

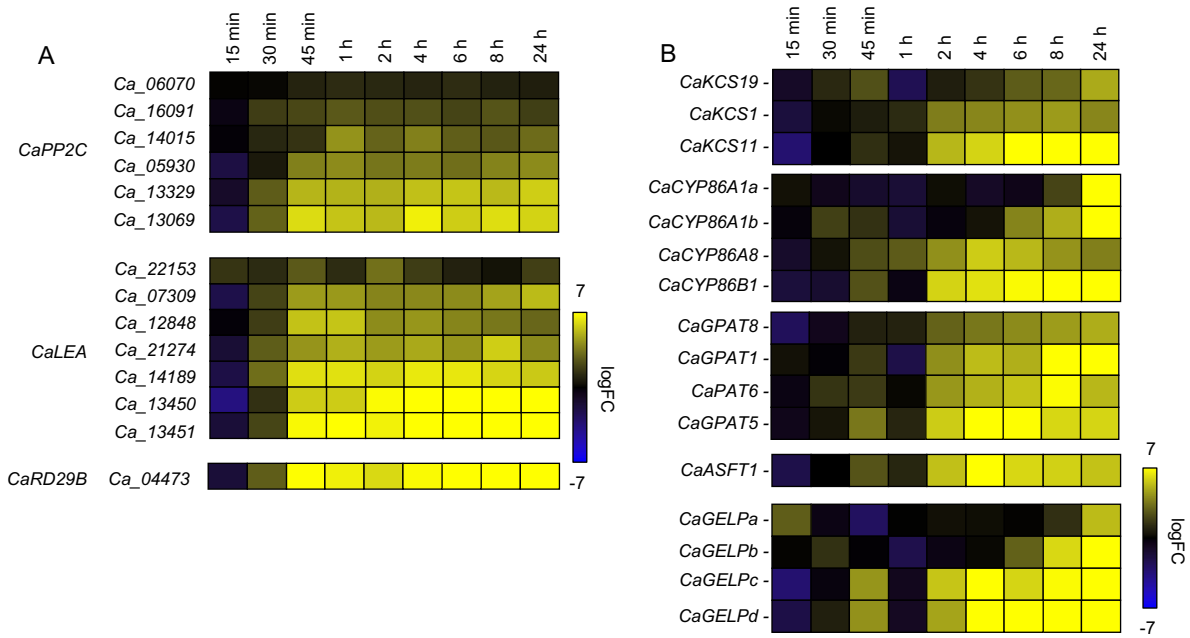

Supplementary Figure S5. Heatmap displaying the logFC values of genes associated with the putative general ABA response (**a**) and suberin biosynthesis and polymerization (**b**) across various time points of the ABA response in chickpea roots when compared to mock treatment.

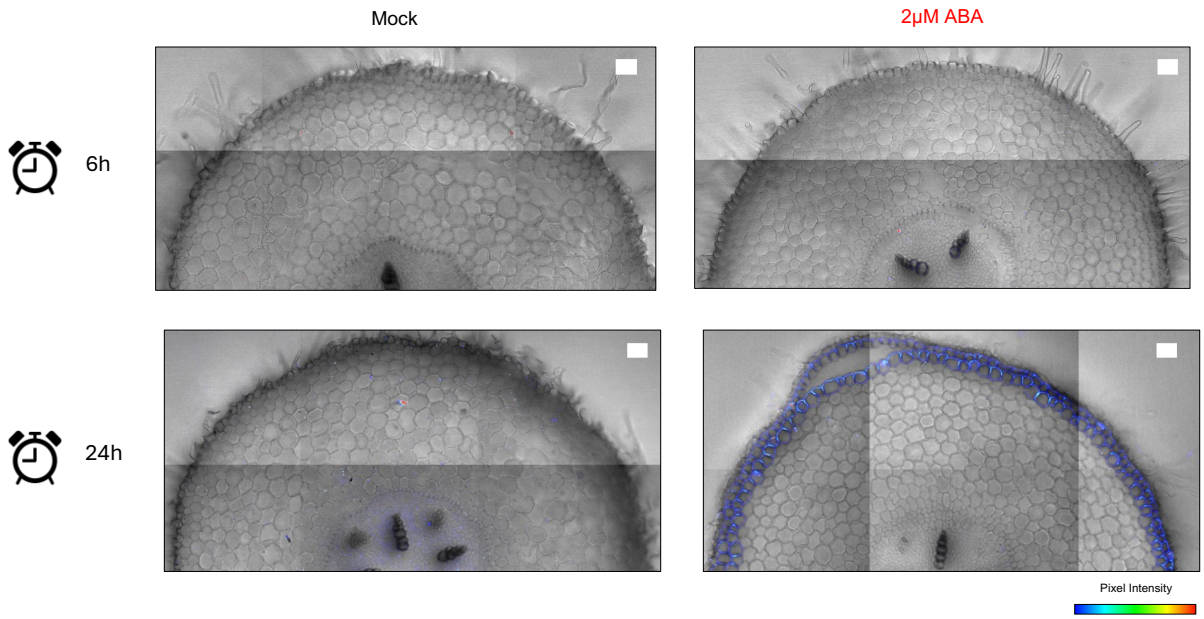

Supplementary Figure S6. Representative confocal images of cross-sections of roots used for the time course RNA-seq experiment: treated with mock or 2 μM ABA at two distinct time points (6 and 24 hours), with the signal of FY overlaid on top of bright field images (scale = 100 μm).

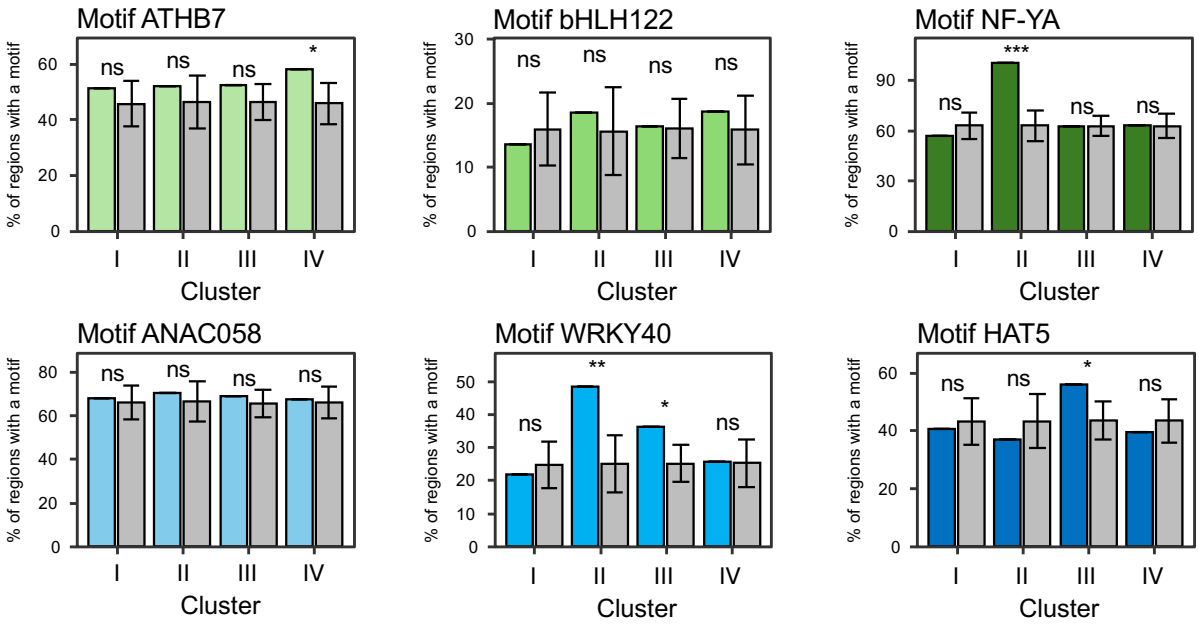

Supplementary Figure S7. Enrichment of ATHB7 (ATNATTG), bHLH122 (CNACTTG), NF-YA (CCAAT), ANAC058 (CNTNNNNNNNANG), WRKY40 (TTGACT) and HAT5 (AATAATT) DNA binding motifs in the promoters of DEGs in clusters I, II, III and IV. Bar graphs show the percentage of promoters of DEGs (colored) and 1000 sets of promoters of randomly selected genes with equivalent number in the compared DEG list (grey) containing the indicated DNA motifs. A Bonferroni-adjusted P-value threshold of 0.01 was used to indicate the statistical significance (*) of enrichment, while ns indicates no significance.

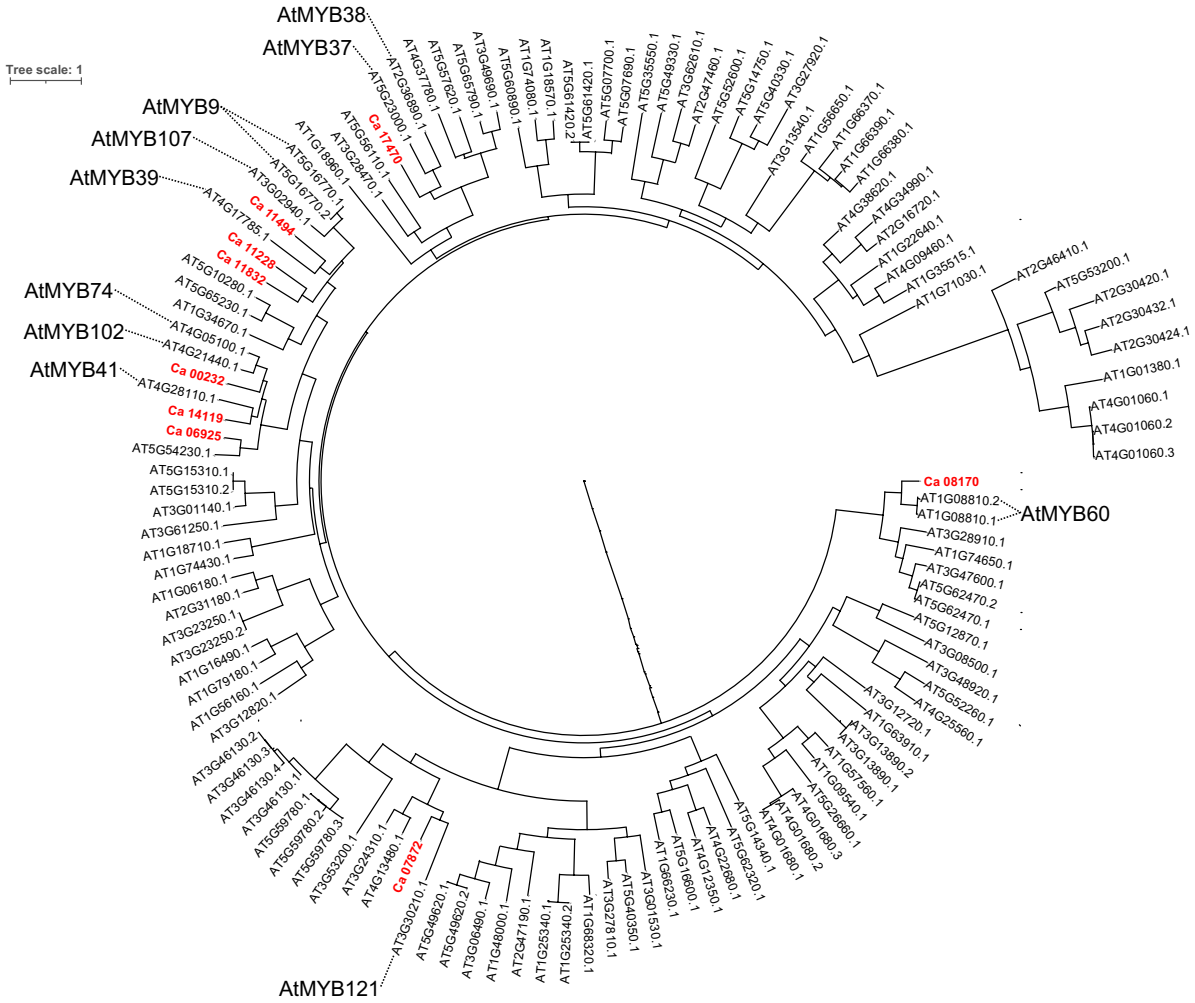

Supplementary Figure S8. Representative phylogenetic tree showing the closest Arabidopsis homologs to chickpea MYBs TFs identified as upregulated by ABA in the time course bulk RNA-seq experiment. Full length amino acid sequences of chickpea upregulated MYBs and all annotated Arabidopsis MYB TFs were aligned using MAFFT. The phylogenetic tree was determined using the maximum likelihood method with 1000 bootstraps using iQ-TREE. Distant nodes where chickpea MYB TFs were not detected were removed to improve the visualization of the cladogram. Upregulated MYBs are indicated in red, and the TAIR10 symbol respective to close orthologues are indicated.

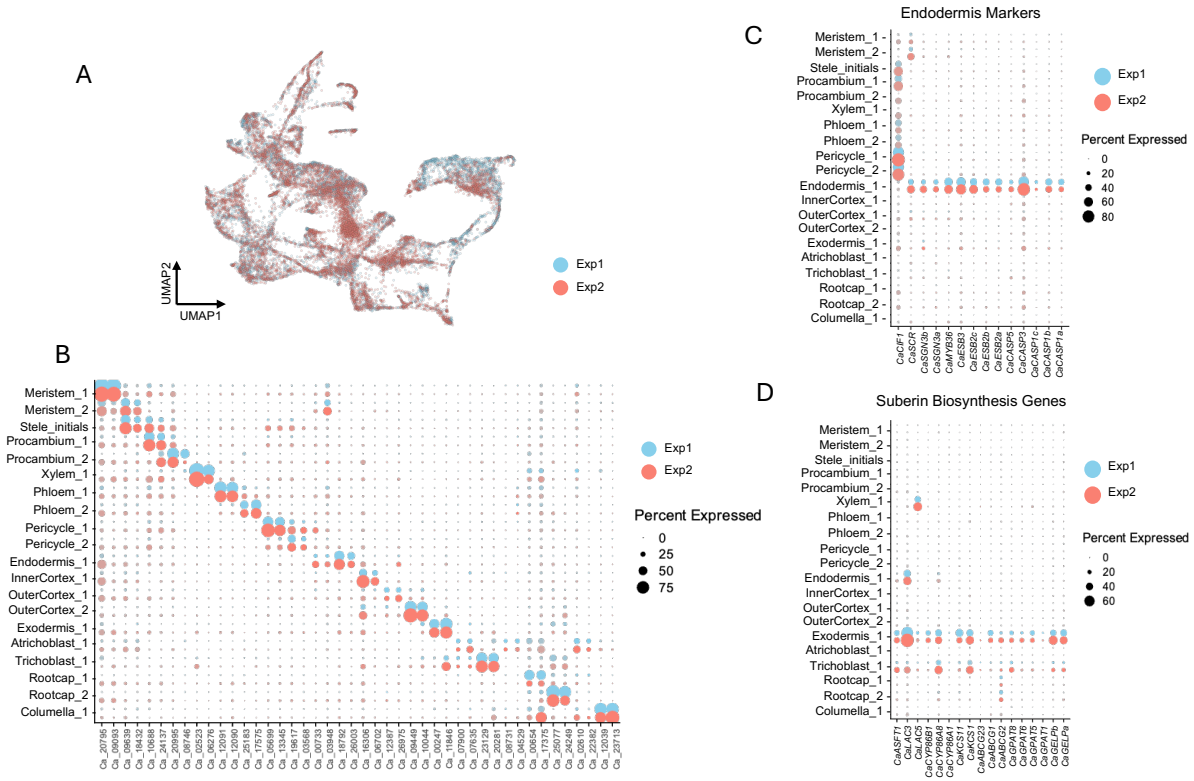

Supplementary Figure S9. Reproducibility of single-cell chickpea root atlas in response to ABA as observed by UMAP (**a**), markers identified (**b**), and profile of expression of Casparian strip related genes (**c**) and suberin biosynthesis genes (**d**). Two independent experiments (Exp1 (blue) and Exp2 (salmon)) that generated individual single-cell libraries from protoplasts isolated from chickpea roots grown in the presence of 2 µM ABA, Exp1 for 24h and Exp2 for 48h. Dot size indicates the percentage of cells in the cluster that expresses the specific gene (% expressed). Dot colours represent the average scaled expression of genes in the clusters (Avg. expression).

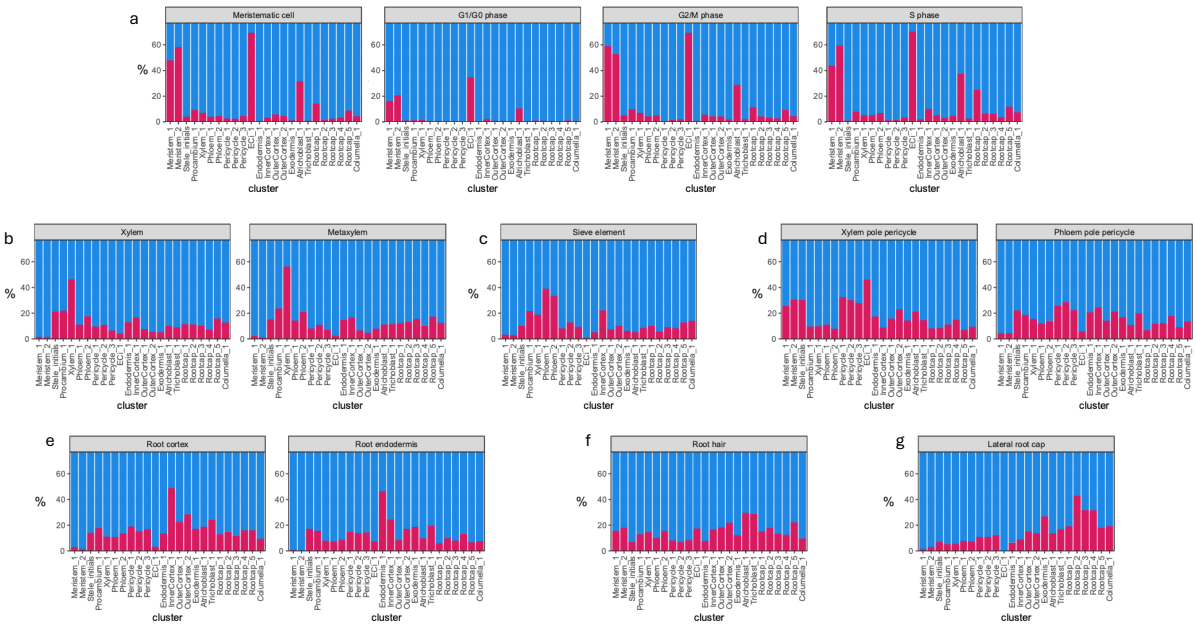

Supplementary Figure S10. Bar plots showing the percentage of chickpea genes in each annotated single-cell cluster that has at least one orthologue identified as a marker in the Arabidopsis root scPlantdb cluster from cell representing dividing cells (a), xylem (b), phloem (c),

pericycle (d), ground tissue (e), epidermis (f) and root cap (g). We manually curated the datasets in the scPlantdb by only keeping datasets in which *AtMYB36* was annotated as a marker for the endodermal cell cluster.

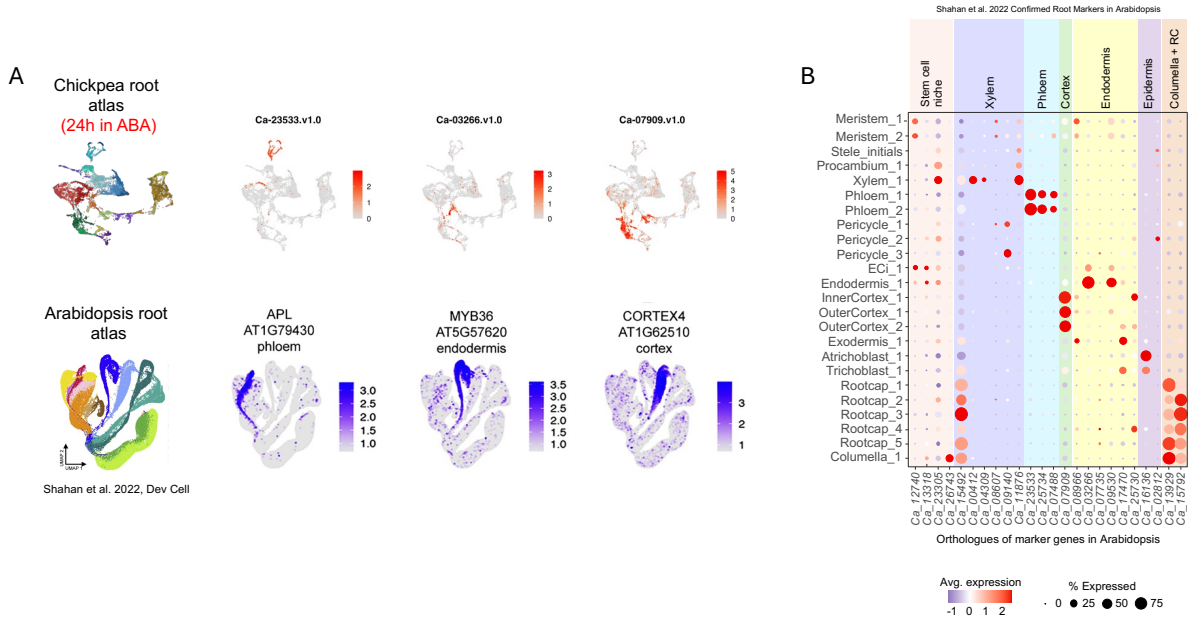

Supplementary Figure S11. a, Top: UMAP profile showing the scaled expression of orthologue genes to characterized markers in Arabidopsis by Shahan et al. 2022. Bottom: UMAP profile showing the scaled expression of marker genes in Arabidopsis phloem, endodermis and cortex[49]. **b**, Dotplot showing the spatial expression of chickpea orthologues of empirically determined root cell markers in Arabidopsis determined by Shahan et al. 2022.

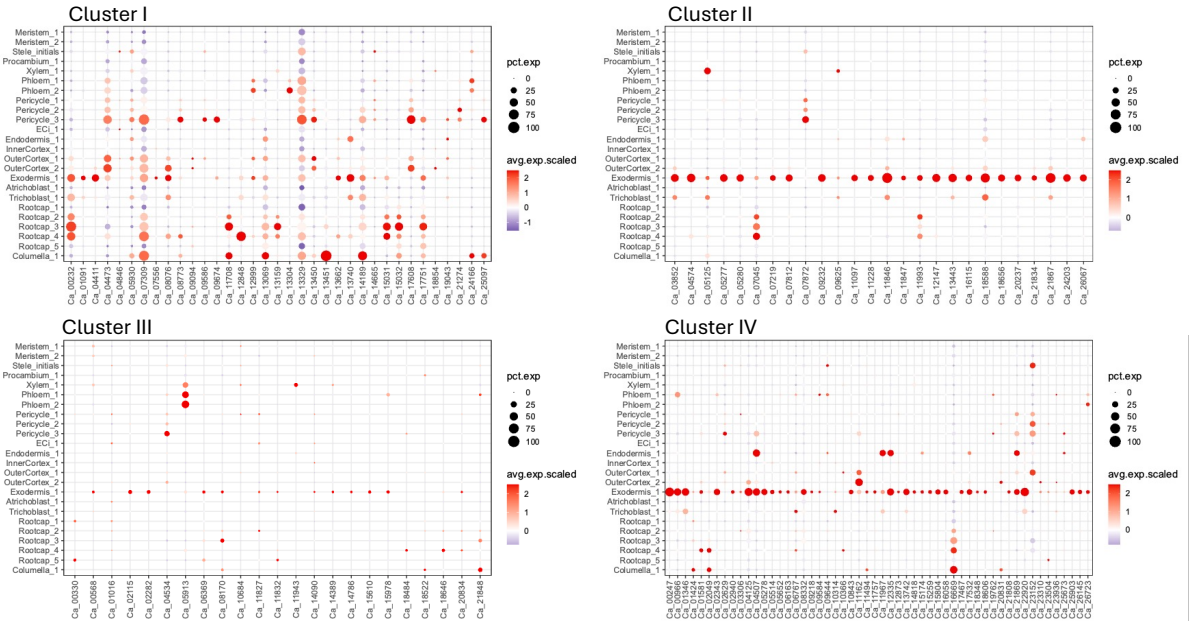

Supplementary Figure S12. Dotplot showing the spatial expression of genes found in Cluster I, II, III and IV, based on the K-means clustering analysis of the time course bulk-RNAseq experiment in chickpea roots in response to ABA.

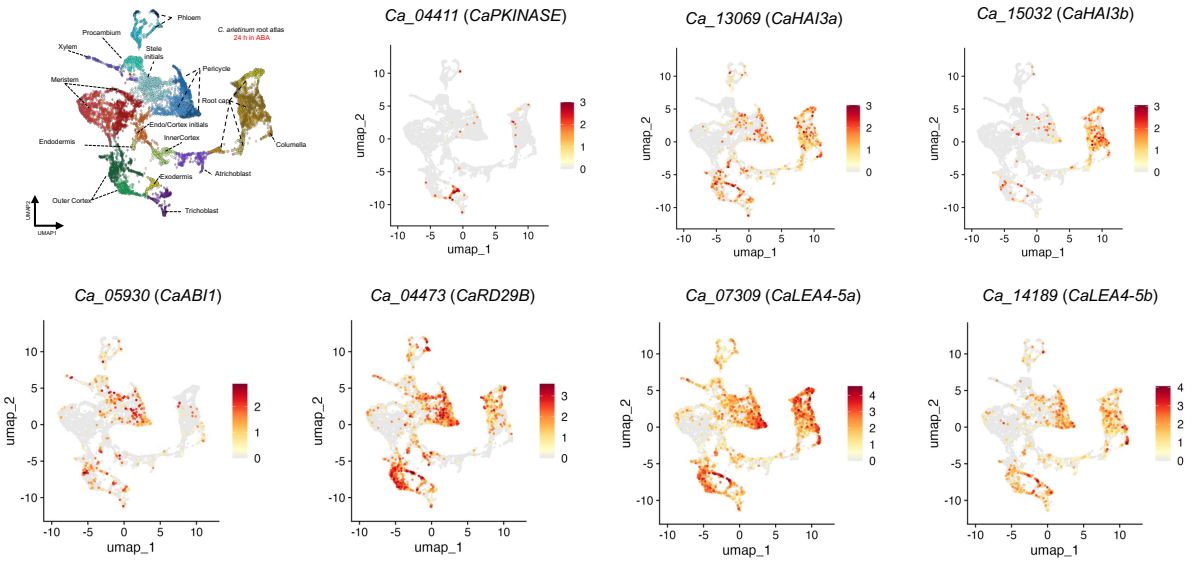

Supplementary Figure 13 UMAP profile showing the scaled expression of select putative ABA responsive genes in the single-cell atlas of chickpea roots grown on 2 μM ABA for 24h.